BNWL-1139
UC-80
4-
2-70

[redacted]

ANALYSIS OF FTR PHASE B CRITICAL EXPERIMENTS PART 2 ZPR-III ASSEMBLIES 52a, b, c, d, e, and f

W. R. Young and R. A. Bennett

February 1970

[redacted]

AEC RESEARCH & DEVELOPMENT REPORT

BATTELLE NORTHWEST
BATTELLE MEMORIAL INSTITUTE PACIFIC NORTHWEST LABORATORIES
BATTELLE BOULEVARD, P. O. BOX 999, RICHLAND, WASHINGTON 99352

BNWL-1139

LEGAL NOTICE

PACIFIC NORTHWEST LABORATORY
RICHLAND, WASHINGTON
operated by
BATTELLE MEMORIAL INSTITUTE
for the
UNITED STATES ATOMIC ENERGY COMMISSION UNDER CONTRACT AT(45-1)-1830

AEC-RL RICHLAND, WASH.

BNWL-1139
UC-80, Reactor
Technology

ANALYSIS OF FTR PHASE B CRITICAL EXPERIMENTS

PART 2

ZPR-III ASSEMBLIES 52a, b, c, d, e, and f

by

W. R. Young

and

R. A. Bennett

Reactor and Plant Technology Department
FFTF Division

February 1970

BATTELLE MEMORIAL INSTITUTE
PACIFIC NORTHWEST LABORATORIES
RICHLAND, WASHINGTON 99352

Printed in the United States of America
Available from
Clearinghouse for Federal Scientific and Technical Information
National Bureau of Standards, U.S. Department of Commerce
Springfield, Virginia 22151
Price: Printed Copy $3.00; Microfiche $0.65

ANALYSIS OF FTR PHASE B CRITICAL EXPERIMENTS
PART 2
ZPR-III ASSEMBLIES 52a, b, c, d, e, and f

W. R. Young and R. A. Bennett

ABSTRACT

Critical experiments in support of the design of the Fast Flux Test Reactor have been carried out in ZPR-III Assemblies 48, 48A, 51, and 52a, b, c, d, e, and f, by personnel of Argonne National Laboratory. This report presents the results and analysis of the experiments performed in Assemblies 52a, b, c, d, e, and f.

TABLE OF CONTENTS

LIST OF FIGURES

LIST OF TABLES

ANALYSIS OF FTR PHASE B CRITICAL EXPERIMENTS
PART-2
ZPR-III ASSEMBLIES 52a, b, c, d, e, and f

W. R. Young and R. A. Bennett

INTRODUCTION

ZPR-III Assemblies 52 are the third series of fast plutonium criticals assembled by Argonne National Laboratory (ANL) for Battelle-Northwest as part of the Fast Test Reactor (FTR) critical experiments program[1,2]. Experimental results have been reported in the monthly ANL Reactor Development Program Progress Reports. These reports will be referenced as the data derived from them is presented.

Assemblies 52a through 52f were fast criticals with central fuel-free regions and with driver and reflector zones that had the same composition as the corresponding zones of ZPR-III Assembly 51[3]. The critical masses of Assemblies 52 ranged from 201 to 309 kg of fissile material. The central fuel-free zones were composed of a mixture of stainless steel and sodium with volumes ranging from 0 to 119 liters.

These assemblies with simulated test zones were devised to check methods for calculating effects of large dilute zones in the FTR and to derive data that can be directly applied to or extrapolated to the design of the FTR.

Critical masses and reaction rate distributions were important parts of these studies. They are important because the total thermal power of the FTR will be limited to 400 MW_t and the "Current Reference Design Value" of the peak flux is 0.73×10^{16} n/cm^2-sec.[4] The design value of the peak flux under the 400 MW limit cannot be assured unless reliable predictions of the critical mass and flux distributions are available for the early design of the FTR. These values are not easily calculated because the large in-core heterogeneities made a three-dimensional core analysis necessary.

SUMMARY

MULTIPLICATION CONSTANT AND CRITICAL MASS

The six assemblies investigated in this series of experiments may be divided into two classes on a geometric basis. Four were slightly irregular, multizoned, right-circular cylinders and two were essentially split-core assemblies. The cylindrical systems with their range of fuel-free central zone volumes were used to infer effective zone bucklings for use in X-Y analyses of the split-core assemblies.

A test zone axial buckling of 4.52 m^{-2} and a core-reflector average axial buckling of 6.85 m^{-2} were used for the analysis. The multiplication constants for these six critical assemblies were calculated with a mean value of $\bar{k}$ = 0.9917 ± 0.001 and ranged from 0.9880 to 0.9962. This consistent underestimate indicates a systematic error arising from either the data set or the calculational model. These calculated eigenvalues are, however, well within the Estimated Current Accuracy (ECA)[5], ±3% Δk/k, and within the "Expected Nuclear Design Uncertainties for the FFTF," ±2% Δk/k[2]. In addition, one may consider these cores, because of their many common features, e.g., composition and general dimensions, to be essentially, a single-type system which may be included with those of an earlier survey[6].

If the correction $k = k_{calc} + 0.0083$ is applied, the k obtained for an additional assembly in this series would be, k = 1.000 ± 0.0025. This uncertainty is within the Target Design Accuracy (TDA)[5] of ±1% Δk/k. The error corresponds to a maximum of ±1.4% ΔM/M for fissile material added at the core edge or ±0.5% ΔM/M for fissile material added evenly over the core.

Uncertainties exist in extending these critical mass results to cores with different fertile to fissile material ratios, different reflectors, or different core spectra. Experience

with ZPR-III Assembly 51 indicates compensating errors in ^{239}Pu and ^{238}U cross sections data[3]. The effect of the compensating errors on critical mass calculations of varying enrichments has not been determined.

Confidence can be gained in applying these results to the FTR because the average fertile to fissile ratio of the two zone FTR is expected to be nearly the same as these assemblies, 4:1. The fuel densities of the FTR driver zone are also expected to nearly match the densities of the core in each of these assemblies. Problems in extending these results to FTR, in general, may arise because of the small platelet heterogeneities of ZPR-III materials in contrast to fairly homogeneous nature of pinned fuel in the FTR. Further problems are connected with large in-core heterogeneities of the FTR. The plate heterogeneity problem has been investigated through the use of flux-volume weighted cross sections. The effect of large in-core heterogeneities will be measured in future FTR critical experiments.

PERIPHERAL POISON ROD WORTHS

A single B_4C (natural boron) rod, 2.7 liters; 18 vol% B_4C, at the core edge of Assembly 52a had a measured worth of 0.207 ± 0.003% Δk/k. Its worth was calculated to be 0.206% Δk/k giving a calculated to experimental ratio (c/e) of 0.995 ± 0.014. This compares with the measurement of the same rod on the axis of Assembly 51, which was calculated with a c/e of 0.917[3]. The worth of this B_4C edge rod may be compared with a 91% enriched B_4C rod in 48A. This rod was worth 0.42% Δk/k and calculated to a c/e of 1.04 to 1.07[7].

A single tantalum rod, 2.7 liter, 18 vol% Ta, at the core edge of Assembly 52a was measured to be worth 0.117 ± 0.002% Δk/k. Its worth was calculated to be 0.142% Δk/k giving a c/e of 1.213 ± 0.021. The same measurement on a central rod in Assembly 51 gave a c/e of 0.935[3].

Calculation of the worth of the natural B_4C poison drawer is well within the "Recommended, Expected Nuclear Design Uncertainties" for the FFTF of ±20%[2]. The tantalum worth fits the criteria marginally.

The B_4C rod worth is within the ECA for "Global"[5] perturbations of ±40% and the TDA of 15%. Tantalum rod worth falls only within the ECA.

FISSION RATE DISTRIBUTIONS

Shapes of the spatial distributions of ^{239}Pu fission rates are calculated better in the core than in the reflector. Near core-reflector boundaries the calculation of fission distributions is not reliable because of the uncertainty in resonance absorptions and the shift in neutron spectrum.

Axial reaction rate distributions along a sodium filled central column are not predicted well in the core or reflector. The code calculates a monotonically decreasing reaction rate distribution that differs greatly from the actual measured distribution. These results imply that axial power density calculations of dilute test zones in the FTR may be in considerable error and should be used with caution. The inferred error in axial peak-to-average power is ±5%.

A linearly averaged peak-to-average radial flux ratio in 52d, the slotted core, was inferred from measurement to be 1.173 ± 0.004 and calculated as 1.30. The calculated to experiment ratio, c/e is 1.11. The same parameters in 52f, a quasi cylindrical core with a central test zone, gave a c/e of 1.04. The 7% variation between these two radial traverses is due to the DB^2 approximation for axial leakage in the X-Y calculation for 52d. R-Z geometry was used in the 52f calculation making the axial leakage directly calculable.

DESCRIPTION OF ZERO POWER REACTOR III (ZPR-III)

The facilities of the ZPR-III at the National Reactor Testing Station, Idaho Falls, Idaho are owned by the United States government and operated, under contract with the U.S. Atomic Energy Commission, by Argonne Laboratories. Detailed descriptions of the facility have been published[8].

Briefly, the ZPR-III can be described as a split table critical facility. Reactor materials are loaded as flat plates, typically 1/8 to 1/4 in. thick. The plates are placed in long drawers that fit into horizontal matrix tubes. One matrix cell is made up of a matrix tube, the drawer, and the drawer contents. A matrix cell is, on the average, 2.182 in. high by 2.178 in. wide.

ZPR-III ASSEMBLIES 52, MATERIAL DENSITIES

CORE MOCKUP OF FTR DRIVER

The material densities of the cores of Assemblies 52 approximated those of the driver zone of the FTR. The core material of the criticals, except for eight safety drawers and two control drawers, was contained in drawer types designated A and A*, whose loadings of materials are shown in Figure 1 and average compositions are listed in Table 1.

RADIAL REFLECTOR

The nickel-sodium radial reflector had a drawer loading of three nickel plates per sodium filled can or about 17 vol% Na, 62 vol% Ni and 12 vol% 304 SS. This composition should be compared to the present concept of the FTR reflector of 64 vol% metal and 35 vol% sodium. Atom densities of the radial reflector are given in Table 1. The drawer loading, as viewed from the front of half I, is shown in Figure 1.

TABLE 1. Assembly 52 - Average Compositions
Atom Density (x 10^{-24} cm^3)

Drawer Type	$^{239-241}Pu$	$^{240-242}Pu$	^{235}U	^{238}U	Mo	Na	C
Core Type A	0.001972	0.000170	0.000012	0.005703	0.000224	0.010262	0.003113
Core Type A*	0.001498	0.000175	0.000018	0.008306	0.000431	0.008244	0.003113
Control Rod	0.001990	0.000162	0.000015	0.007144	0.000197	0.010123	0.002746
Light Safety Rod, 52a,b,c	0.002990	0.000329	0.000032	0.014635	0.000796	0.004039	0.000916
Heavy Safety Rod, 52d,e,f	0.000902	0.000119	0.000012	0.005705	0.000224	0.010340	0.004150
Radial Reflector	---	---	---	---	---	0.00416	---
Axial Reflector	---	---	---	---	---	0.010321	---
Test Zone	---	---	---	---	---	0.016335	---

	O	Al	Fe	Cr	Ni	Mn	Si
Core Type A	0.011479	0.000110	0.01521	0.003783	0.001655	0.000158	0.000185
Core Type A*	0.014093	---	0.01000	0.003530	0.001544	0.000147	0.000173
Control Rod	0.008241	0.000124	0.016047	0.003992	0.001747	0.000167	0.000196
Light Safety Rod, 52a,b,c	0.005362	0.000026	0.017198	0.003829	0.001675	0.000160	0.000188
Heavy Safety Rod, 52d,e,f	0.017212	---	0.016122	0.003561	0.001558	0.000149	0.000175
Radial Reflector	---	---	0.007605	0.00187	0.0564	---	0.00009
Axial Reflector	---	---	0.010426	0.002583	0.028926	0.000182	0.000120
Test Zone	---	---	0.013044	0.003245	0.001420	0.000136	0.000159

AXIAL REFLECTOR

The axial reflectors have three nickel plates per five sodium filled cans. The resultant composition is 41 vol% sodium, 32 vol% nickel and 16 vol% stainless steel. Atom densities are listed in Table 1, while the drawer loading, as viewed from the front half I, is shown in Figure 1.

TEST ZONE

The test zone drawers of Assemblies 52 had only sodium filled cans. The composition was about 64 vol% sodium, 21 vol% stainless steel. The composition of the test regions is found in Table 1. A drawing of platelets in this drawer is not shown since it contains only sodium filled cans.

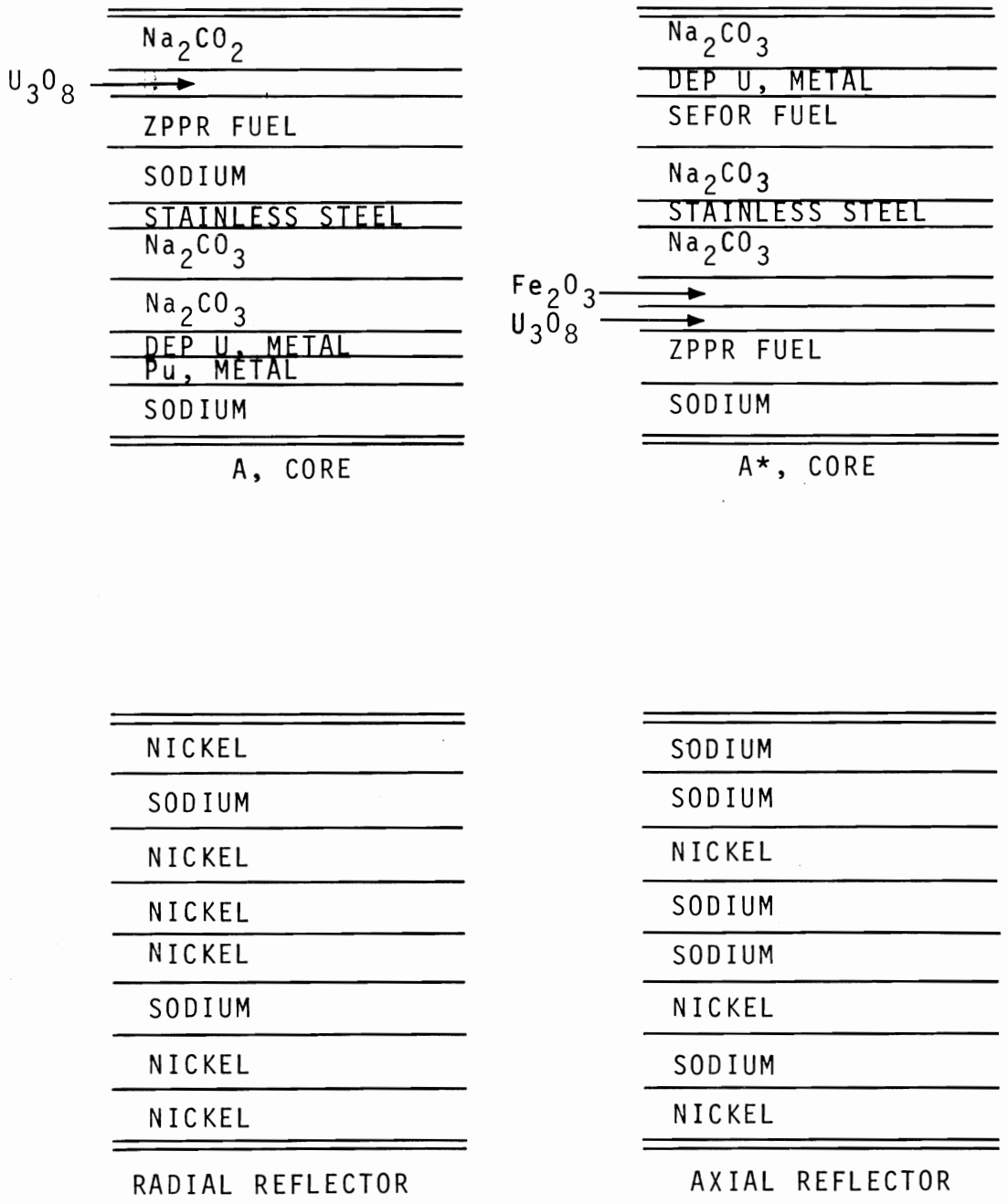

FIGURE 1. Drawer Loadings for ZPR-III, Assemblies 52

SAFETY DRAWERS

A safety requirement for ZPR-III operation is that a total of 1.5% $\Delta k/k$ of reactivity must be held in the safety drawers.[9] This was achieved in Assembly 52 by placing safety drawers in matrix positions which normally would be occupied by A* drawers. For Assemblies 52a, b, and c additional fuel was added in the form of an 1/4 in. thick SEFOR fuel column; 1/4 in. thick ZPPR fuel column, and a 1/8 in. thick U_3O_8 column to each A* drawer loading used for the safety drawer in order to bring their total worth to 1.5%. This fuel replaced two 1/4 in. thick $NaCO_3$ cans, a 1/8 in. stainless steel plate and a 1/8 in. depleted uranium plate. Note that 5/8 in. of material replaced 3/4 in. of material of a normal A* loading. The other 1/8 in. goes into the drawer walls of safety drawers. The drawer loading, of the eight safety drawers (for Assemblies 52a, b, and c), is shown in Figure 2.

Assemblies 52d, e, and f required more fuel in the safety drawers to achieve the required shutdown margin. The Fe_2O_3 plate of the light loading was replaced with a plutonium metal plate. This loading, the heavy safety drawer loading, is also depicted in Figure 2, while the atom densities of these safety drawer loadings are given in Table 1.

The major difference between Assemblies 51 and 52a was the method of safety drawer spiking. Fuel for spiking the safety rods of 51 came from neighboring A* drawers such that the average composition of the core was identical with an unspiked core.[3] In contrast to Assembly 51, fuel was added to the safety drawers of 52a without a corresponding decrease of fuel in neighboring drawers. The result was an increase in the average concentration of ^{239}Pu in 52a of 4% over an unspiked assembly.[10,11] The increased concentration resulted in a critical mass that is 8 kg less than the corresponding Assembly 51 configuration.

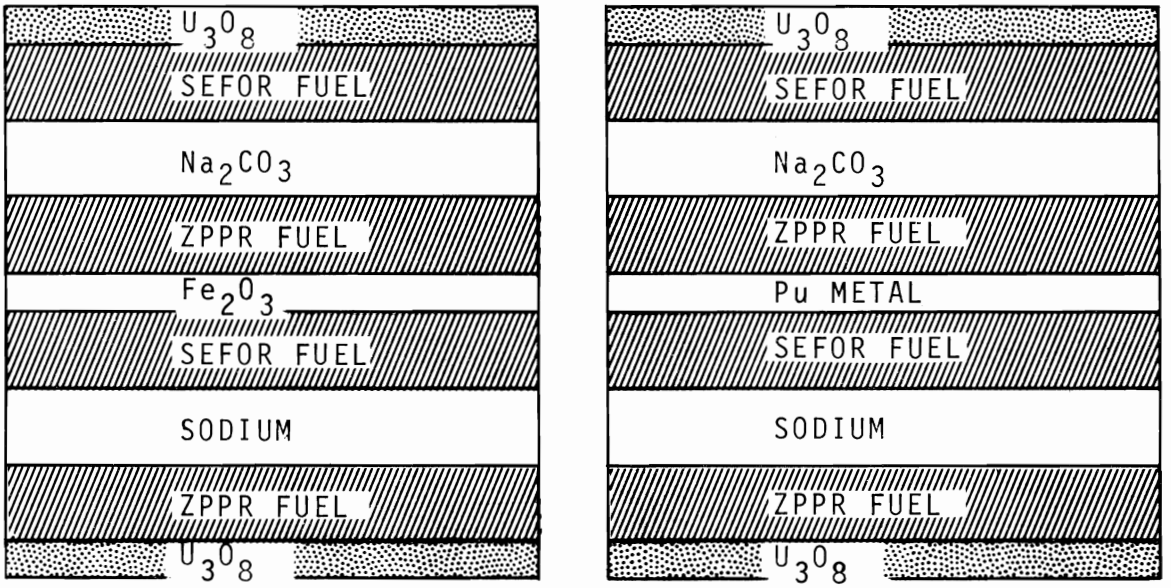

FIGURE 2. Assemblies 52 Safety Drawer Loadings

Measurements were made on the reactivity effect of spiking the safety drawers of Assembly 52e. These measurements, on two safety drawers, predict an increase of 2650 Ih* will accompany the spiking of eight safety drawers in 52e.[12] Using calculated edge worths for 52e, this increase in k corresponds to about 36 kg of fuel removed from the core edge. The increase in fissile fuel concentration and consequent decrease in the critical mass are undesirable because they make analysis more difficult and decrease the relevance of the experiment to the FTR design.

*1% $\Delta k/k$ = 1036 Ih[11]

EXPERIMENTAL RESULTS AND ANALYSES

Critical masses, fission rate distributions, and single peripheral poison rod worths were measured and analyzed as part of the Assembly 52 experimental series. Critical mass was measured for each of the six assemblies while peripheral poison worths were measured only in the right cylinder, 52a, and fission rate distributions were measured only in the cores 52d and 52f.

Analyses of experiments were done with the data sets and computer codes presently in use for the physics design of the FFTF. The basic cross section data, including resonance self shielding factors and temperature dependencies, are from a modified version of the 26 group Bondarenko set.[13,14] The energy structure and fission source distribution of the 26 group set are given in Appendix A.

Both diffusion and transport theory were used in the analyses reported. The specific computer codes used were:

FCC-IV	Reference (15)
DTF IV (modified)*	" (16)
2DB	" (17)
2DF	" (18)
PERT-IV	" (19)

For most calculations of effective multiplication constants, a convergence criterion of 10^{-5} was specified which yields an eigenvalue converged to within $\pm 5 \times 10^{-5}$ $\Delta k/k$. Mesh points were two to four cm apart in interior core regions and four to five cm

The modifications only extend to using the DTF IV transport calculated fluxes for peripheral calculations such as flux-volume weighting and collapsing cross sections and certain reaction rate calculations.

apart in the reflectors. Near zone boundaries they were separated by less than 1 cm. Typical mesh structures for a two-dimensional calculation contained between 500 and 900 spatial mesh points.

CRITICAL MASS

The face maps of the cores are shown in Figures 3 through 8. All cores were 34 in. high and nominal 12-in. thick radial and axial nickel-sodium reflectors. The test zones ran the full height of the core and through the axial reflector.

Drawer inventories of the assemblies are given in Table 2. The assembly may be supercritical with the fissile inventory listed in Table 2 because the control rods may be only partially inserted. If this is the case, a small mass must be subtracted from the masses listed in Table 2 to bring the Assembly to critical. If the reactor is slightly subcritical with the control drawers completely inserted mass must be added to the fissile inventory. In all cases, the corrections were less than 1 kg of fissile. The corrected critical masses along with the calculated eigenvalues are listed in Table 3.

The measured critical mass of each assembly is known only to within ±0.5 kg because core edge fuel worths were not measured. As a consequence these cores were not cylindricized in the same manner as Assembly 51. Cylindricization of Assembly 51 was done by using measured drawer edge worths for drawers A and A* at various radii. An empirical curve for each drawer worth was inferred from these measurements as a function of distance from the center. The centroid of each volume added or subtracted was assumed to be the radius of the mass and its worth was read from the curves.

A further uncertainty in the measured critical masses is in the fissile content of platelets. ANL estimated this uncertainty to be ±0.5%.[20] This uncertainty has been added to the

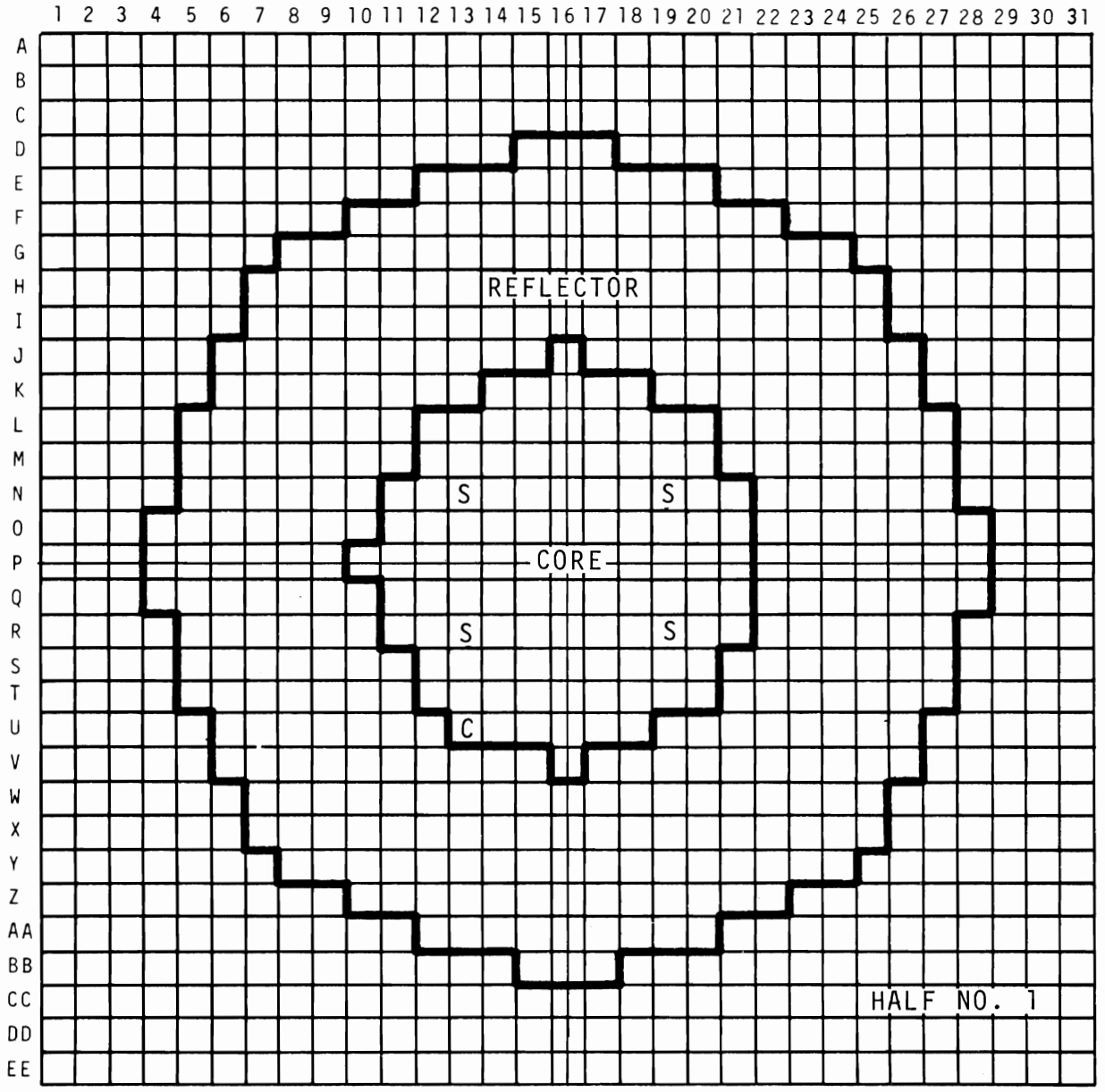

FIGURE 3. Reference Loading, Assembly 52a

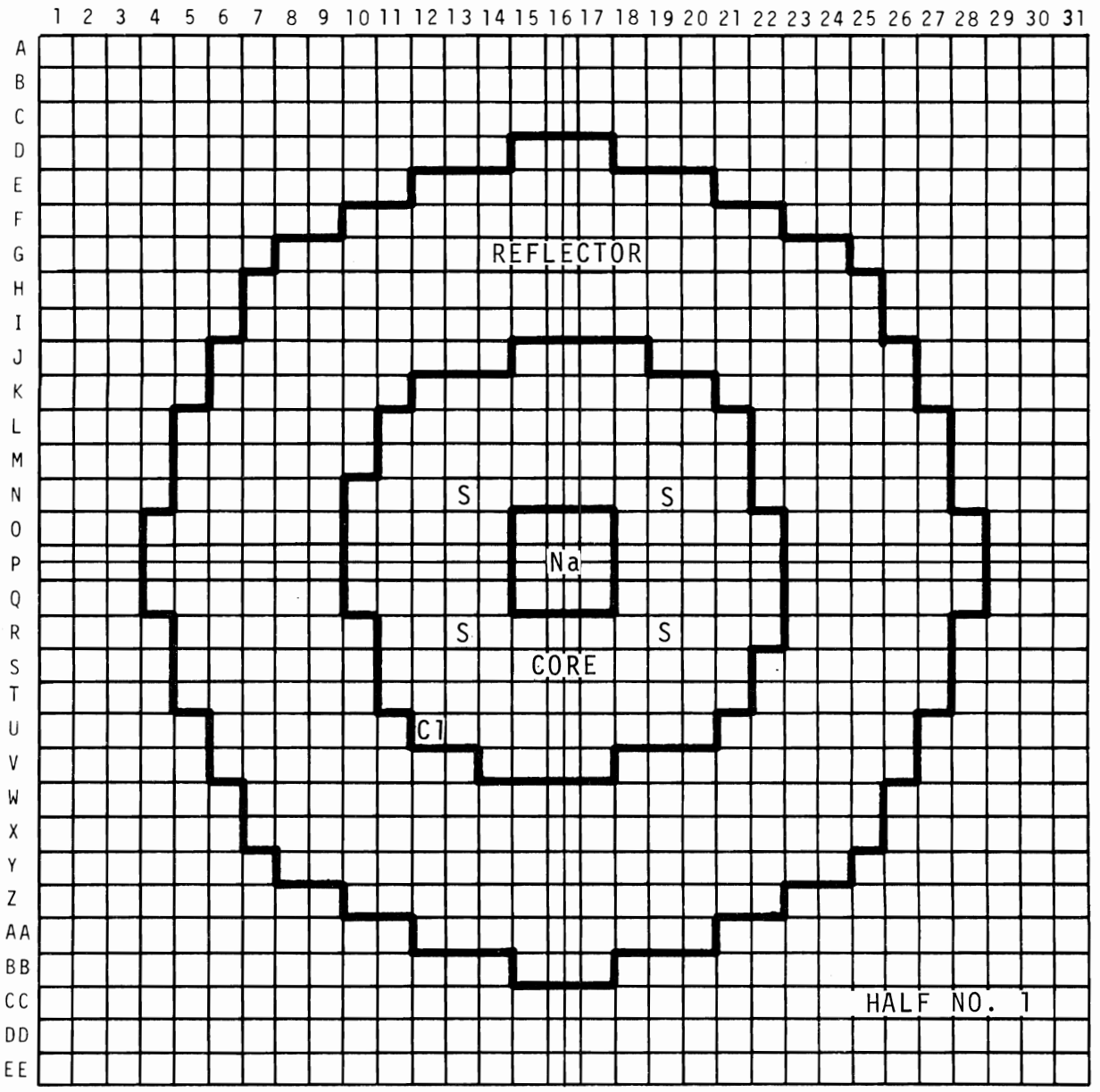

FIGURE 4. Reference Loading, Assembly 52b

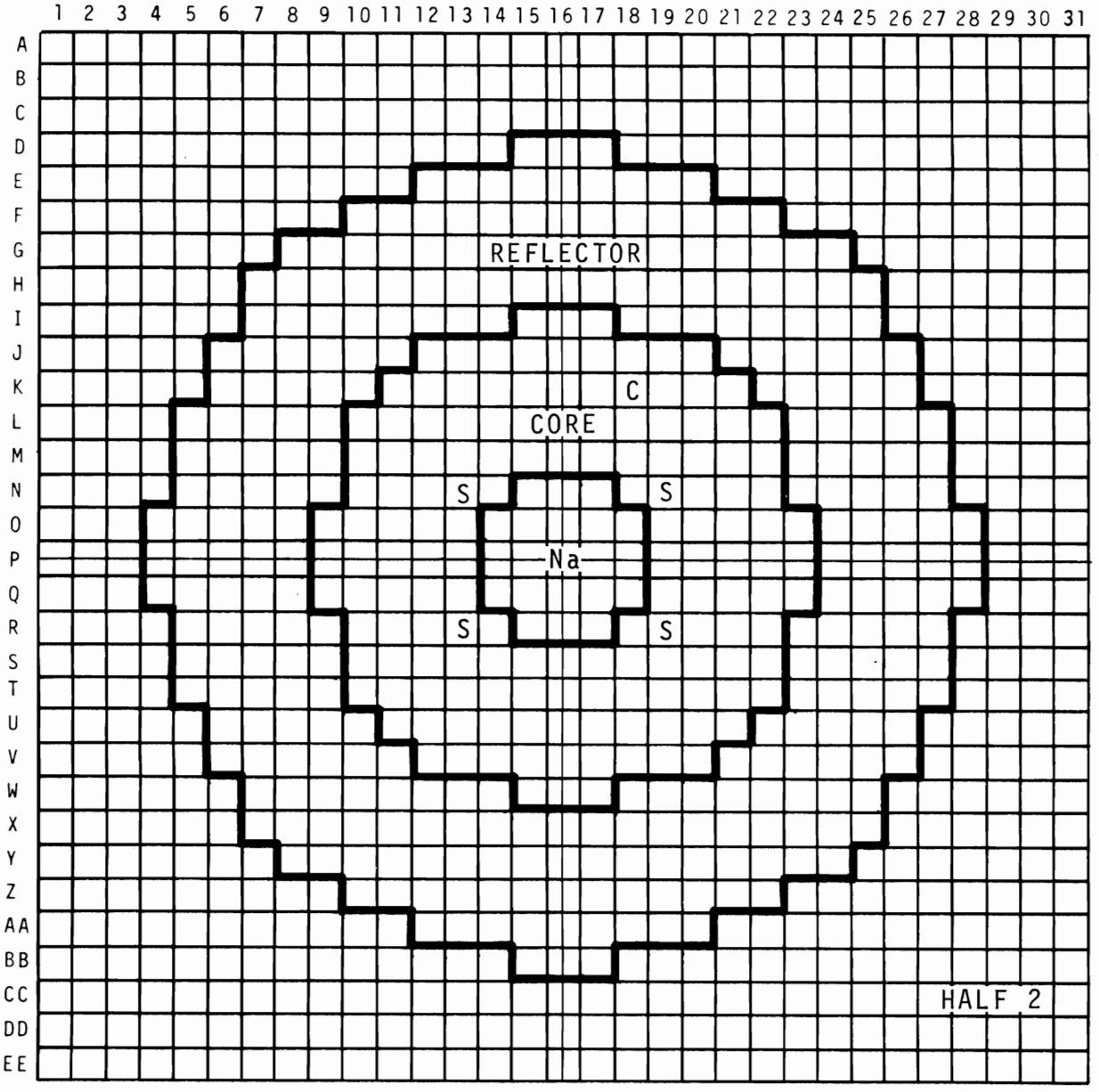

FIGURE 5. Reference Loading, Assembly 52c

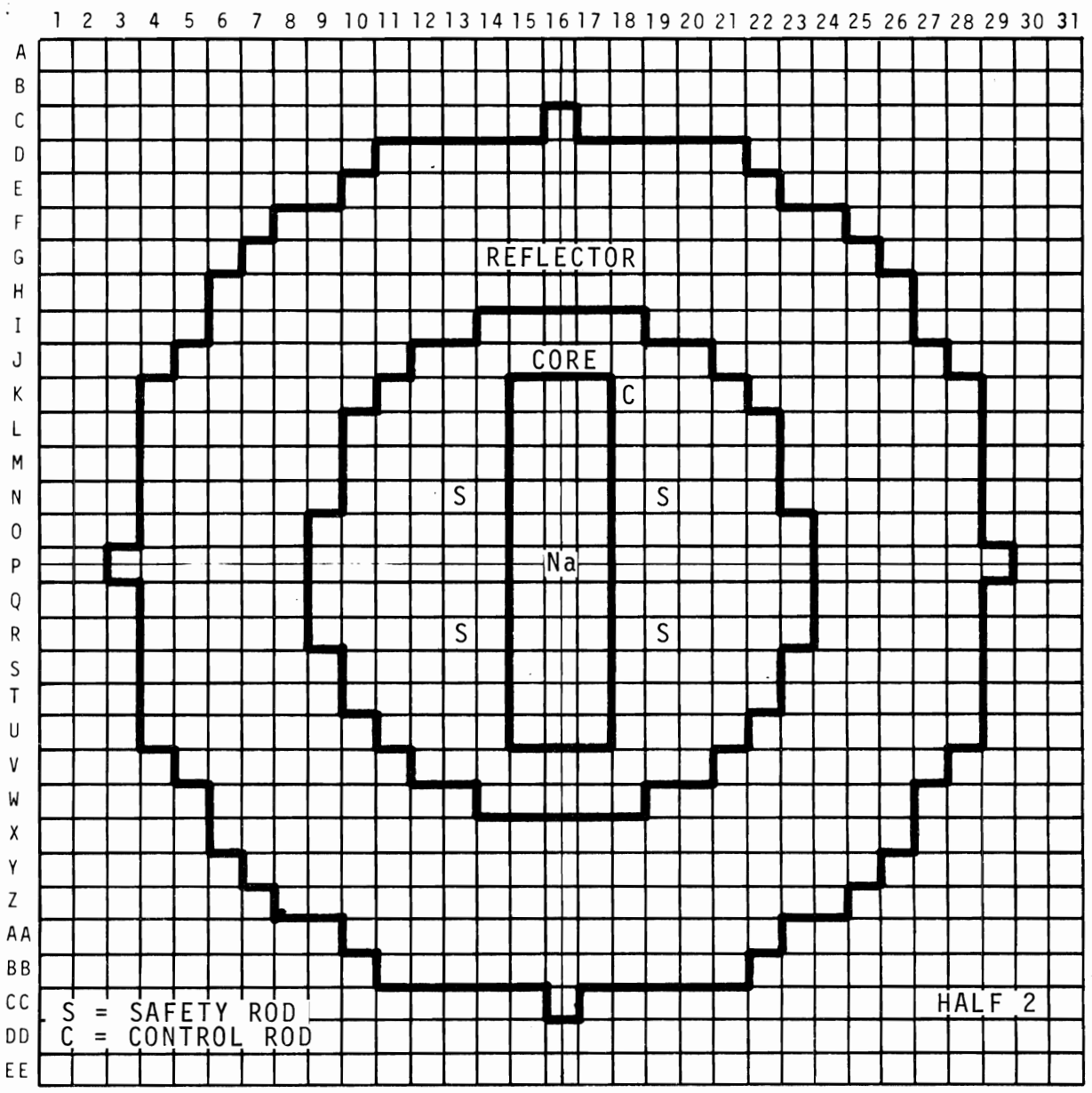

FIGURE 6. Reference Loading, Assembly 52d

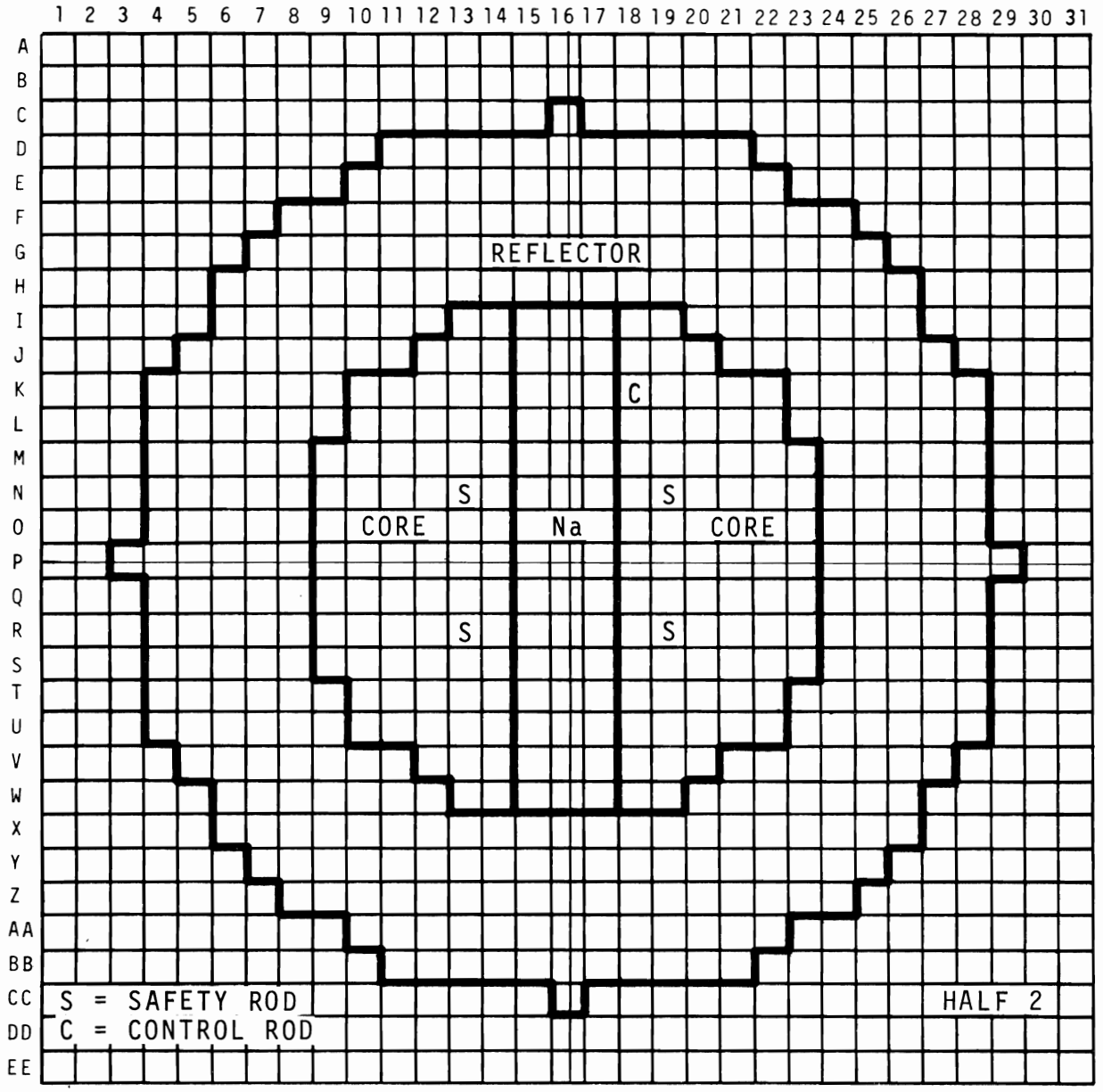

FIGURE 7. Reference Loading, Assembly 52e

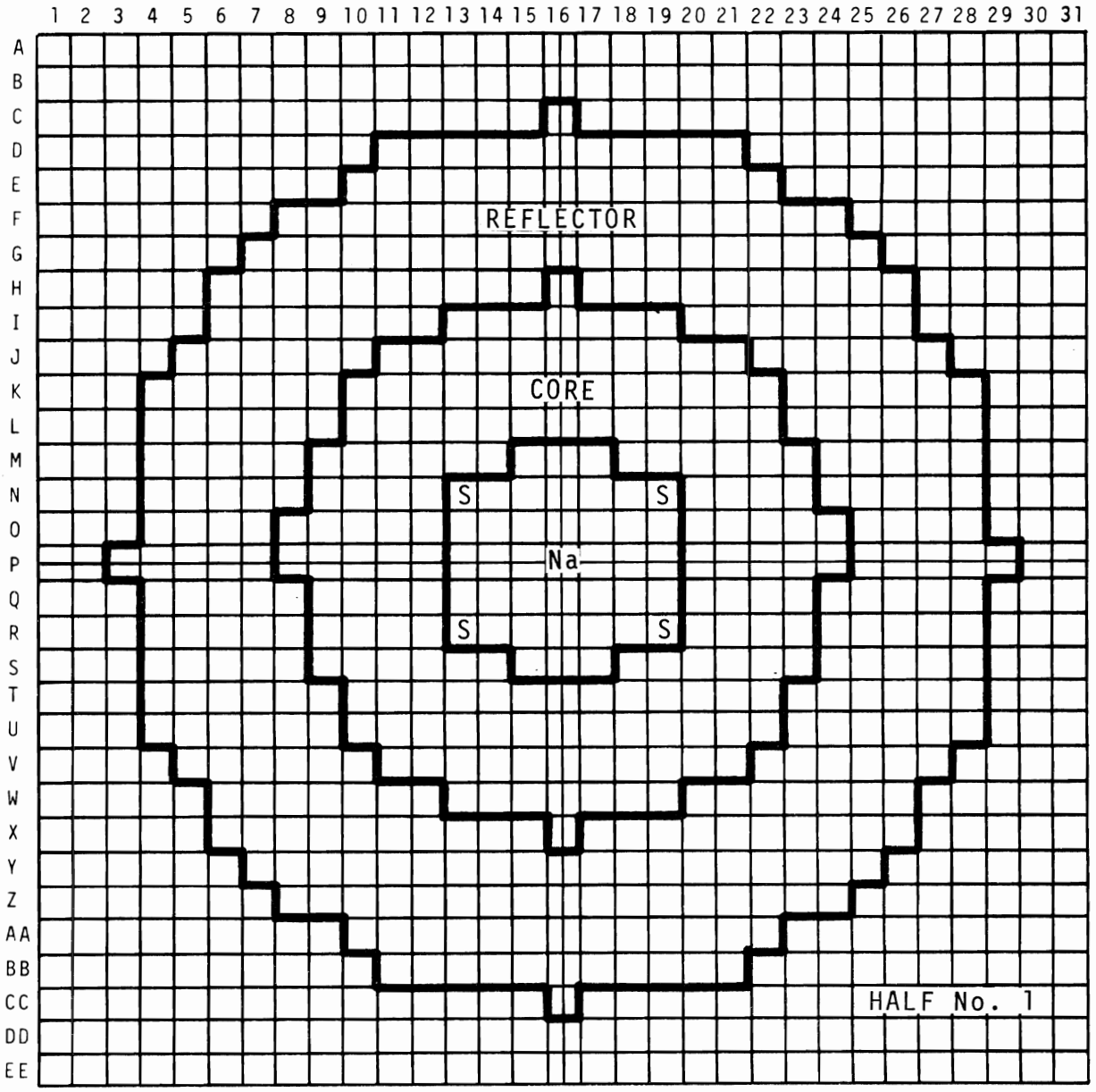

FIGURE 8. Reference Loading, Assembly 52f

TABLE 2. Core Drawer Inventories of ZPR-III Assemblies 52[10,12]

Assembly	Core Drawers: Type A[a] Number	Type A[a] Fissile, kg[b]	Type A*[a] Number	Type A* Fissile kg[b]	8 Safety Drawers Fissile, kg[b]	2 Control Drawers Fissile, kg[b]	Totals, kg of Fissile
52a	107	111.82	93	74.21	12.72	1.85	200.6
52b	127	132.72	111	88.58	12.72	1.85	235.97
52c	148	154.67	139	110.92	12.72	1.85	280.16
52d	155	161.98	119	94.96	17.23	1.85	276.02
52e	155	161.98	127	101.35	17.23	1.85	282.41
52f	163	170.34	151	120.50	17.23	1.85	309.92

(a) *A in even numbered columns, A* in odd numbered columns.*
(b) $^{239}Pu + {}^{241}Pu + {}^{235}U$

±0.5 kg that has been quoted as the measured mass assuming a nominal fissile inventory. The total uncertainty is quoted in Table 3 with the result for each core. This corresponds to an error of ±0.004 Δk/k for all cores. A correction for cylindricization of the irregular core outline of Assembly 52a was calculated to be -0.01% Δk/k. This correction will be smaller for the other cores because it diminishes with increasing core size.

The reactor calculations were made with the 2D diffusion theory code 2DB with the 8 energy groups whose structure and fission source distribution shown in Appendix A. Cross sections from the basic 26 group set were prepared with the codes FCC-IV and DTF-IV (modified). A separate FCC-IV run for each assembly region composition at 300 °K was made for the resonance shielding calculations. These calculations were made on an homogeneous model with a Bell[21] correction for resonance absorptions. These 26 group resonance shielded cross sections were collapsed to eight energy groups if they were associated with fuel free zones. If they were associated with fueled zones, the 26 group resonance shielded cross sections were used in a DTF-IV cell calculation where they were corrected for spectral and spatial variations.

TABLE 3. Critical Calculations of Assemblies 52

ZPR-III Assemblies 52	Critical Mass, Experiment,[10,12]	K_{eff} Calculated	
		RZ	XY
a-cylinder	200.7 ± 1.5	0.9898	0.9864
b-24 liter central hole	235.9 ± 1.7	0.9880	
c-66 liter central hole	280.0 ± 1.9	0.9925	
f-98 liter central hole	309.2 ± 2.0	0.9959	
d-88 liter rectangular hole	275.2 ± 1.9		0.9878
e-119 liter slotted core	282.0 ± 1.9		0.9962

The cell calculations for flux-volume weighting cross sections were done for the A, A* and the safety drawers. They have been described in the report on ZPR-III Assembly 51[3] and will not be elaborated on here.

The effective multiplication constants for quasi-cylindrical Assemblies 52a, b, c and f were calculated in R-Z geometry. These had core zones that were approximately right cylinders with one spiked safety drawer pair per quadrant. The spiked safety drawers were treated as an annular zone with material and volume equivalent to the four safety drawer pairs. The center of the annulus coincided with the radial point of the center of the safety drawer. This model gives a good approximation to the statistical weight of the added fuel.

This cylindricization was checked by comparing an R-θ calculation with an X-Y calculation. The X-Y calculation gave an eigenvalue that was 0.01% $\Delta k/k$ larger than the R-θ calculation. The increment in Δk is caused by a combination of effects. The smooth boundary and the single smeared control drawer of the R-θ model combined with the irregular boundary, A-A* drawer distribution and discrete four control drawer pairs of the X-Y model gave this very small change in k.

The R-Z calculations were used to infer the axial leakage of the split Assemblies 52d and 52e. Axial buckling for each

quasi-cylindrical core was inferred by running a 1D cylindrical calculation where radial mesh points of the core coincided with the radial core mesh points of the R-Z run. The 1D calculations were searches for an axial buckling that yielded the eigenvalue of the corresponding R-Z calculation. The results are listed in Table 4. It was first assumed that the axial buckling of the core-reflector in each of these assemblies was 6.85 m^{-2}. The test zones and core reflector were each given a statistical weight based upon a flux squared importance. These were equated to the total core buckling and solved for the test zone buckling. The test zone bucklings were then plotted against test zone volume. This curve, when extrapolated to zero test zone volume, gives an inferred buckling of the test zone of 4.52 m^{-2}. A plot of the curve is given in Figure 9.

The above method of buckling determination, where the buckling is extrapolated to zero test zone volume, is appropriate because the axial buckling, 6.85 m^{-2}, describes a particular ratio of core statistical worth to radial reflector statistical worth. This ratio is that of Assembly 52a.

The correct bucklings for the core-radial reflector zone of 52d and 52e were estimated from the core to radial reflector volume ratio by assuming that the correct average buckling for the core plus the reflector depends upon the ratio of the volume of the core to the volume of the reflector. The eigenvalues of these two assemblies were calculated with 2DB in X-Y geometry with a 4.52 m^{-2} as the test zone buckling and 6.85 m^{-2} as the core-reflector buckling. They were then corrected for the deviation of the core-reflector buckling from 6.85 m^{-2}. The corrections were +0.0007 $\Delta k/k$ for 52d and -0.0004 $\Delta k/k$ for 52e.

TABLE 4. Axial Buckling for Cylindrical Approximations

Assemblies 52	Whole Assembly Axial Buckling, m^{-2}
a	6.85
b	6.58
c	6.39
f	6.31

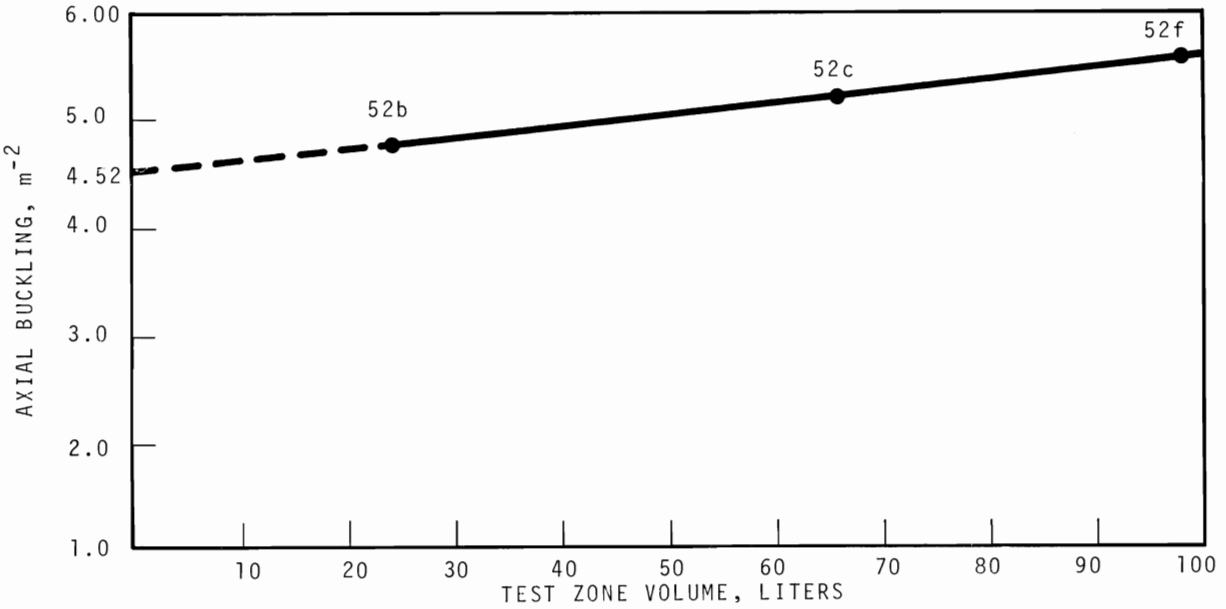

FIGURE 9. Effective Test Zone Buckling for Assemblies 52b, 52c, and 52f

Argonne National Laboratory in analyzing the Assembly 52 series deduced an effective buckling for each of the test zones of the series assuming a constant core-reflector buckling and iterating between X-Y calculations and cylindrical calculations for a test zone buckling. They used an average of the cylindrical core test zone bucklings, 5.0 m^{-2}, for Assemblies 52d and 52e[22]. These values are shown in Table 5 along with the BNW values.

TABLE 5. Axial Buckling Comparisons

Assembly No.	Effective Buckling, B_2^2 m^{-2}			
	Core + R. Refl.		Test Zone	
	BNW	ANL[22]	BNW	ANL[22]
52a	6.85	6.72		
52b	6.85	6.72	4.77	5.31
52c	6.85	6.72	5.15	4.69
52d	6.82	6.72	4.52	5.00
52e	6.87	6.72	4.52	5.00
52f	6.85	6.72	5.46	4.97

Cylindrical calculations using 2DB R-Z were compared with 2DF S4 R-Z transport calculations for Assembly 51[3]. These results, in conjunction with a study by O'Dell, Little, and Hardie,[23] were used to infer the transport correction for the 52 series cores. The transport corrections, 1.0% $\Delta k/k$ for 52a and 0.9% $\Delta k/k$ for the other cores, are listed on the calculational summary for each core in Appendix B.

The effective multiplication calculation range from a maximum of 0.0132% $\Delta k/k$ for 52d to 0.0031% $\Delta k/k$ low for 52e. The corresponding range in overcalculation of the critical mass is 15.5 kg, 7.7% $\Delta M/M$, for the 52a X-Y calculation to 17 kg, 6.1% $\Delta M/M$ for the 52d X-Y calculation. R-Z calculations range from an overcalculation of 11.6 kg, 5.8% $\Delta M/M$ for 52a to an overcalculation of 6 kg, 1.9% $\Delta M/M$ for 52f. In the case of R-Z calculations, this is within the Estimated Current Accuracy (ECA) of ±6% in critical mass stated in the LMFBR Program Document.[4] The X-Y calculations exceed these criteria but always such that they underestimate k by 0.5 to 1.2%. Correcting for this would put all future calculations on assemblies this size and of similar composition within the ECA.

The differences in the accuracy of the calculated eigenvalues for the two slotted cores 52d and 52e reflect the uncertainty in the buckling of the various zones in these cores. The deviation of k as calculated for Assemblies 52d and 52e is ±0.004 Δk/k from their mean value. This corresponds to an error in the axial buckling of the core-reflector of about ±0.2 m^{-2}.

PLUTONIUM FISSION RATE DISTRIBUTION

Fission rate traverses were made in assemblies 52e and 52f with a brass filled ^{239}Pu fission counter. The counter was mounted on a stainless steel carriage assembly and traversed through a 5/8 in. OD SS tube.[12] The counter, traverse tube and carriage assembly were described in the reports for Assembly 51.[3,24]

Calculations of ^{239}Pu fission rate distributions were made with the 2D diffusion code 2DB in eight energy groups. Plutonium cross sections were either core weighted or reflector weighted for reaction rates. Fluxes were derived from the 2DB eigenvalue calculations where cross sections were weighted as described in Section 5.1. Reflector weighted cross sections were prepared using reflector compositions for resonance shielding, infinite dilution of ^{239}Pu, and fundamental mode calculated reflector spectra for collapsing from the 26 groups to 8 energy groups.

ASSEMBLY 52e, SPLIT CORE, FISSION RATE DISTRIBUTIONS

This assembly is only approximately handled by 2D reactor codes. It roughly consists of two axially split halves of a cylinder separated by about 6 in. of sodium and stainless steel (Figure 7). Radial fission rate traverses were calculated in X-Y geometry.

As an aid in evaluating the calculated flux distributions in the split-core FTR three fission rate traverses were made in 52d. An axial traverse down drawer P16 and two radial traverses 1 1/4 in. from the reactor midplane in Rows P and L were made.

The axial traverse was down a sodium-filled drawer whose loading is shown in Figure 10. The fission rate is shown in Figure 11. The statistical counting errors are less than 0.5%, a deviation that is smaller than the plotted points size. Since this traverse was on the assembly axis it was never in core material or reflector material but the traverse was entirely in the SS-sodium simulated test zone. The core and reflector boundaries have been included to show what material is radially adjacent to the test zone at the axial position of measurement.

It is apparent that there is a small maximum coincident with the axial core-reflector interface. This indicates that core leakage neutrons predominate in the test zone adjacent to the core and that reflector leakage neutrons predominate in the test zone outside the core.

The peak-to-average fission rate linearly averaged over the axial traverse in the core was inferred from the measurement to be 1.12.

Radial fission rate distributions are plotted in Figures 12 and 13. Radial fission rates traversed drawers whose loadings are shown in Figure 14. The uncertainties due to statistical variations of count rates are less than 1.0%. They are less in magnitude than the scale spanned on the ordinate by the plotted point.

The shape of the radial fission rate distribution of ^{239}Pu is calculated well in the core and test zone but begins to deviate near the core reflector boundary. These difficulties in reaction rate calculations at the interface are caused by uncertainties in the resonance self-shielding factors of the activation cross sections and the spectral variation there. Activations were calculated for both core and reflector weighted cross sections.

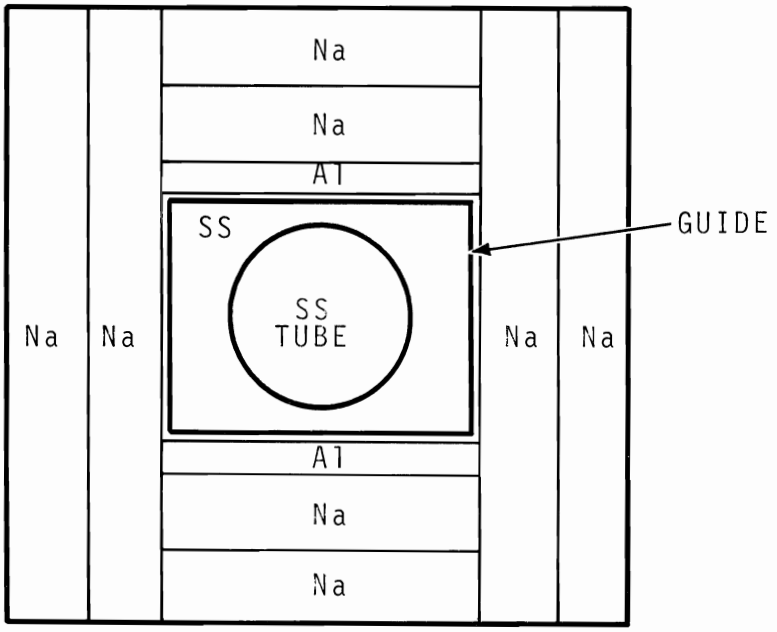

FIGURE 10. Axial Traverse Drawer Loading in Assembly 52e (Front view)

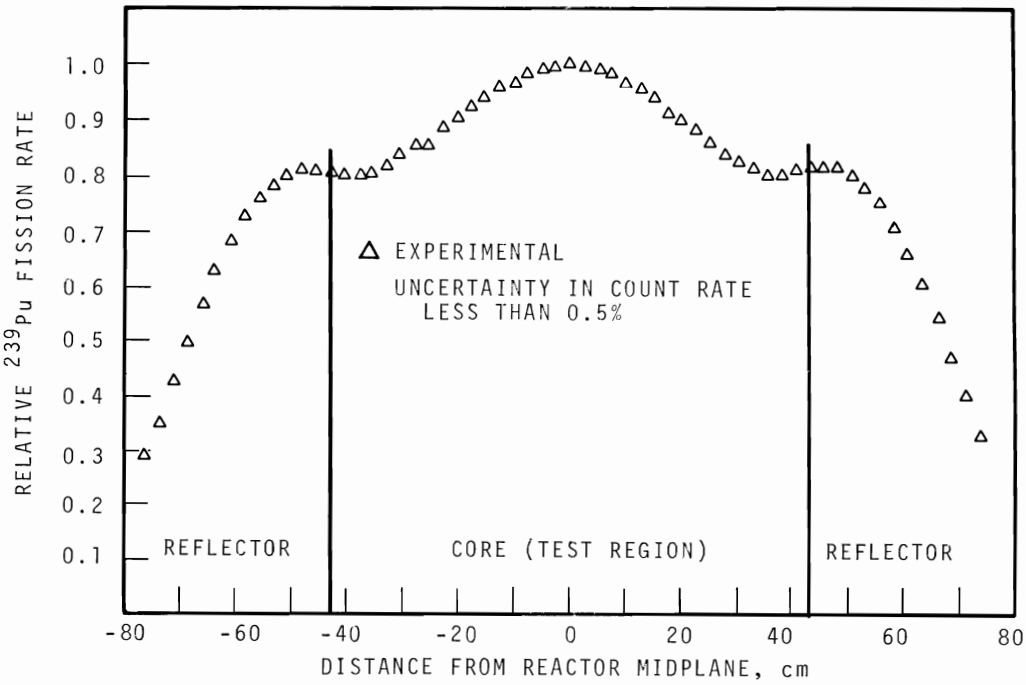

FIGURE 11. Assembly 52e Axial ^{239}Pu Fission Rate Traverse

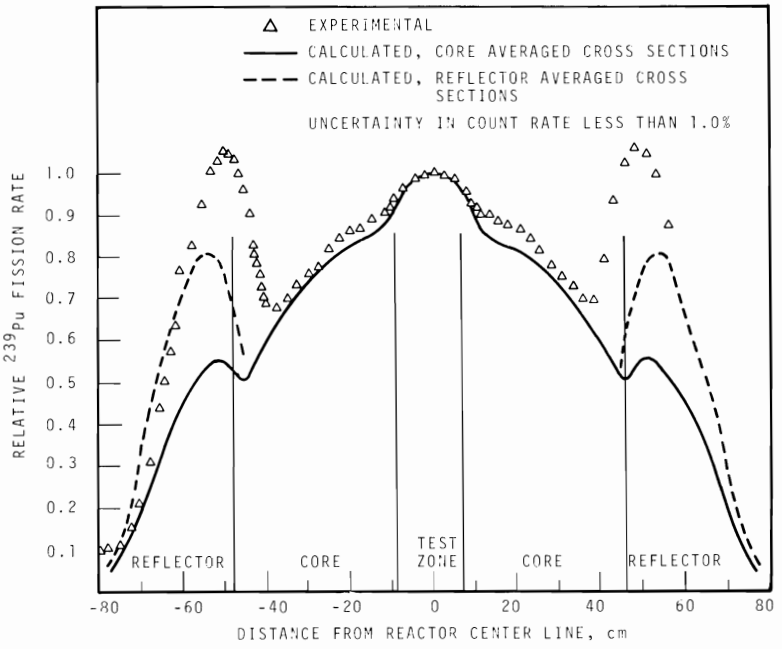

FIGURE 12. Assembly 52e P-Row Radial ^{239}Pu Fission Rate Traverse

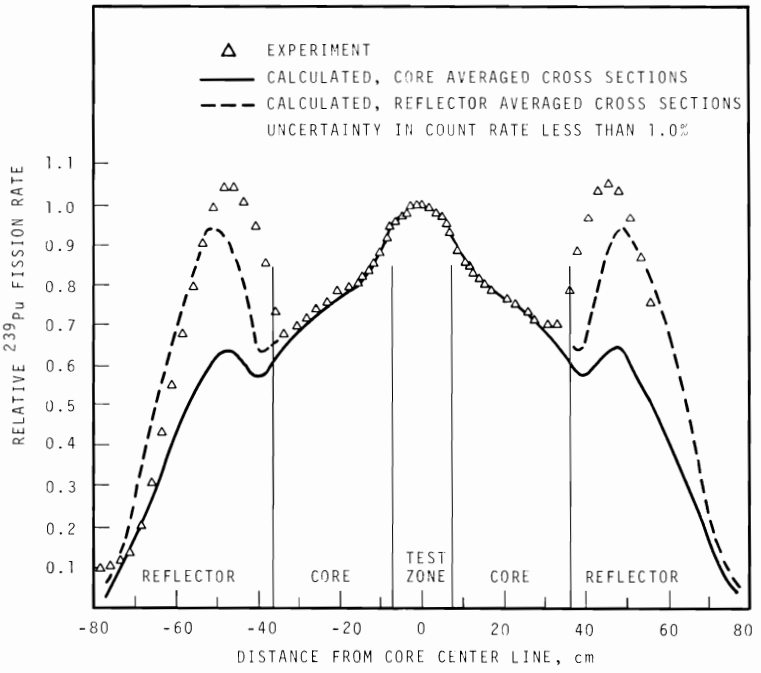

FIGURE 13. Assembly 52e L-Row Radial ^{239}Pu Fission Rate Traverse

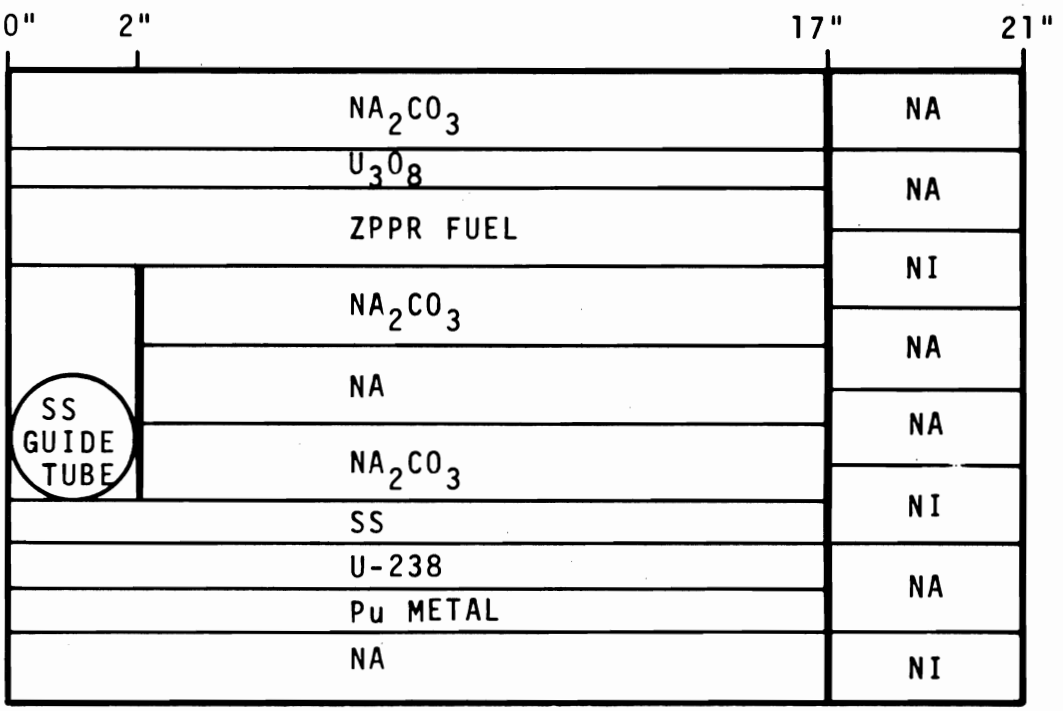

A DRAWER

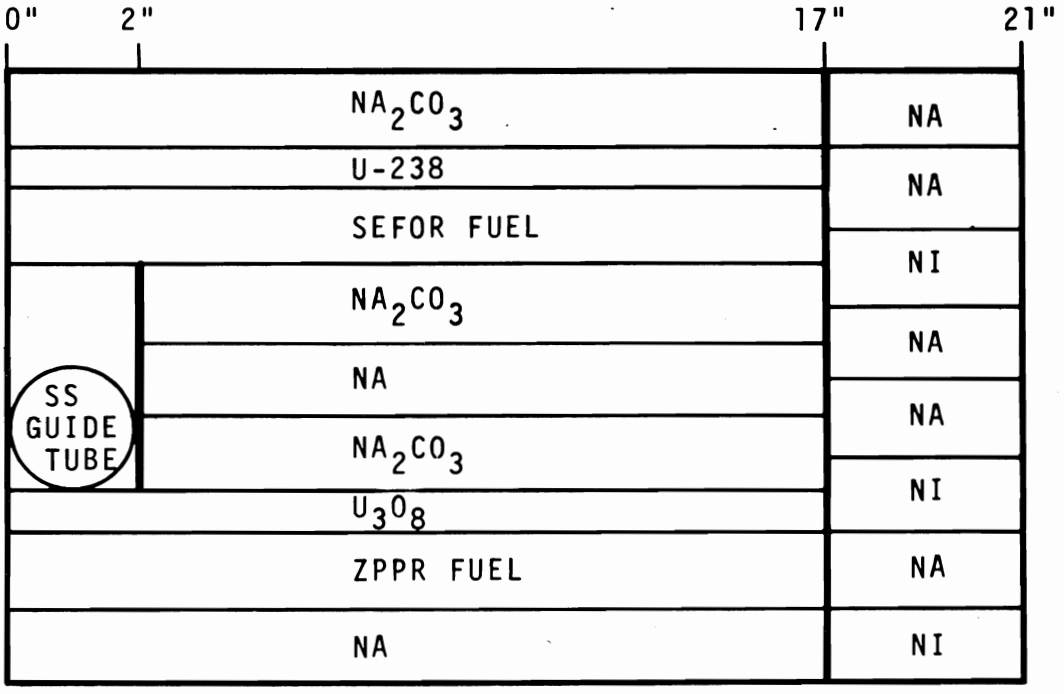

A* DRAWER

FIGURE 14. Drawer Loading for Radial Traverses

Calculated fission rate distributions in the radial reflectors for both the P and L row traverses are low in relation to the center point activities. Assuming that the center point spectrum is correctly calculated it can be concluded that the calculated reflector spectrum is too hard.

The P-row radial ^{239}Pu fission rate distribution measurement was linearly averaged over the traverse path and compared with a calculated average. Linear averaging was used in this case because more traverses or questionable extrapolations would be needed to obtain a measured volume average over this split core, 52d. The peak-to-average fission rate distribution was inferred from measurement to be 1.173 ± 0.004 and calculated as 1.30. The calculated to experiment ratio is 1.11 ± 0.004.

ASSEMBLY 52f, LARGE CENTRAL "HOLE", FISSION RATE DISTRIBUTION

Assembly 52f can be satisfactorily cylindricized (Figure 8) such that an R-Z calculational model can be devised. This obviates finding an axial buckling for each zone of a multizone assembly and simplifies calculations.

Axial ^{239}Pu fission rates were measured through drawer P16 while radial fission rates were measured across Row P.[25] The P16 drawer loading to accommodate the axial traverse tube is shown in Figure 10. Drawer loadings to accommodate the radial traverse tube are shown in Figure 14.

The plots of the fission rate activation are given in Figures 15 and 16. The statistical errors in count rates are less than 0.9% and smaller in size than the plotted point.

Calculated ^{239}Pu fission distributions are obviously poor for the axial distribution down the central test zone. The surrounding region spectrum affects the test zone more strongly than calculations predict. This is evidenced by the change in slope of the measured distribution at the axial core-reflector

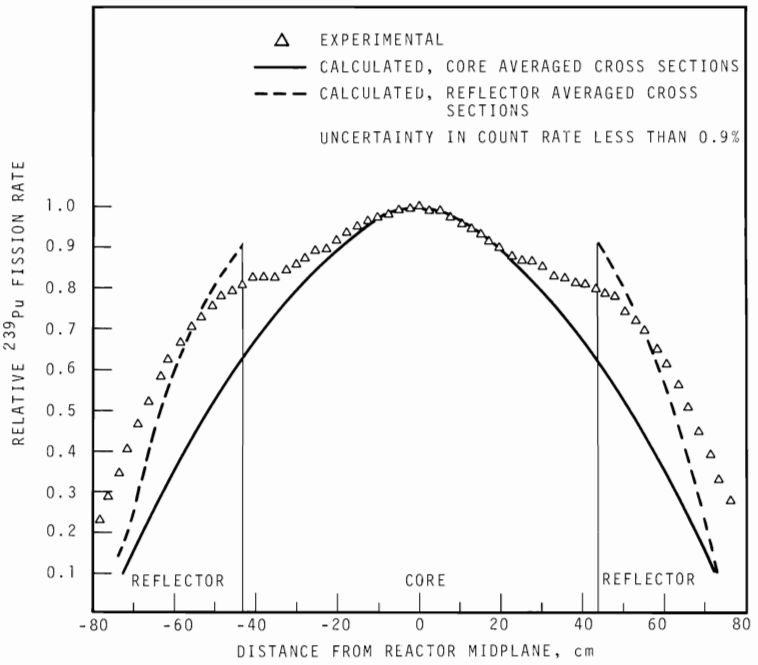

FIGURE 15. Assembly 52f Axial ^{239}Pu Fission Rate Traverse

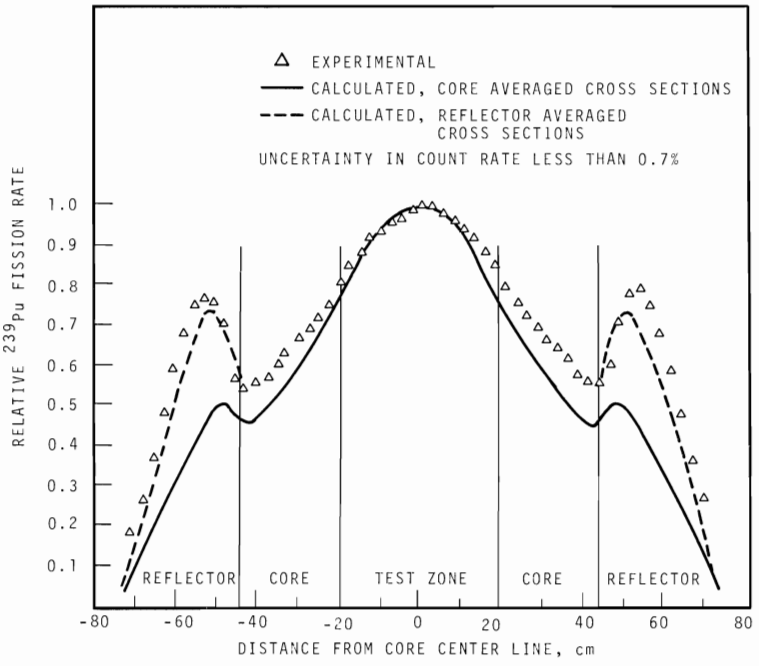

FIGURE 16. Assembly 52f Radial ^{239}Pu Fission Rate Traverse

interface while the slope change is undetectable in the calculated distribution possibly because flux gradients are too great for the diffusion approximation.

Calculated and measured radial in-core fission distributions were calculated with better agreement in Assembly 51 than for this distribution in 52f.[3] Possibly the source of error arises from the large dilute test zone that could influence the core resonance absorptions or the core spectra to cause the discrepancy.

The in-core peak-to-average fission rate was calculated as 1.35 for the radial traverse and 1.17 for the axial traverse. The inferred measurements were 1.30 ± 0.004 and 1.10 ± 0.005. The calculated to experiment ratio, c/e, is 1.04 and 1.05 for the radial and axial traverses, respectively.

The c/e value of the 52d radial fission rate is 6% larger than in 52e. The difference results from the uncertainty in the DB^2 leakage approximation and its effect on the neutron spectra in these cores.

PERIPHERAL TANTALUM AND B_4C ROD WORTHS IN ASSEMBLY 52a

The reactivity worths of simulated B_4C (natural) and tantalum rods were measured in 52a at the core edge in matrix position P22 as shown in Figure 17.[10] The poison drawer inventories are listed in Table 6 and an end view of the drawer loadings are shown in Figure 18. A comparison of the experimental and calculated reactivity changes is given in Table 7.

The c/e of 0.995 ± 0.014 for a B_4C rod may be compared with the same ratio for an identical B_4C rod on the central axis of Assembly 51. This assembly was practically identical to 52a. The calculated to experiment ratio for the central rod was 0.92.[3] The better agreement for the peripheral rod is probably fortuitous and the 8% undercalculation is more representative of the expected error for this calculation.

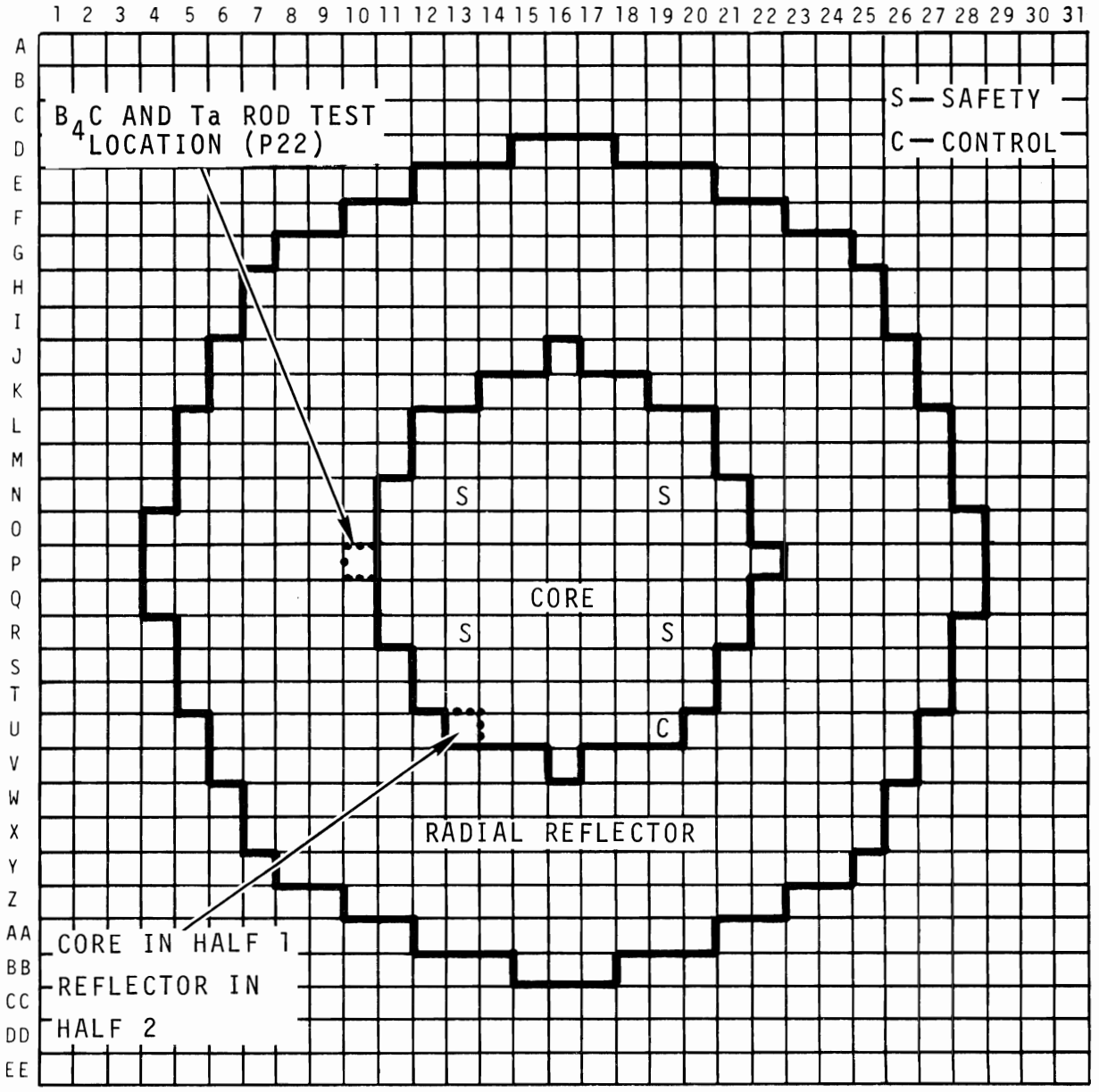

FIGURE 17. Peripheral Rod Worth Assembly 52a

TABLE 6. B_4C and Tantalum Drawer Loadings[10]

		B^{10}, wt%	B^{11}, wt%	C, wt%	Ta, wt%
B_4C	1262.2 g - 96 pieces 1/4 in. × 1/2 in. × 3 in.	13.67	63.31	23.02	0
Ta	9432 g - 72 pieces 1/8 in. × 2 in. × 2 in.	0	0	0	100.0

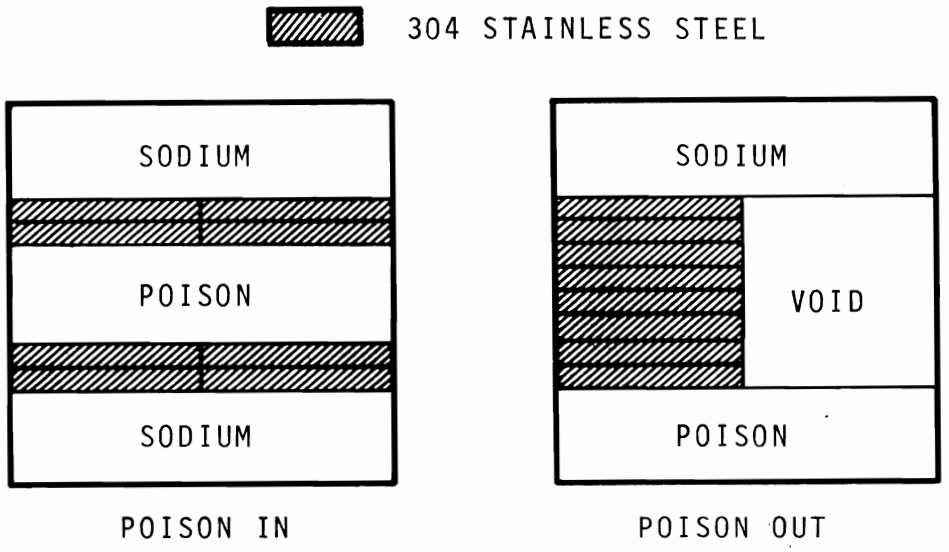

FIGURE 18. Drawer Loading for B_4C and Tantalum Studies

Correlations with Assembly 48A calculational accuracy for peripheral B_4C rods are of limited value because the 48A rods were 91% enriched in B-10, 690 g/rod, compared with 13 wt% B-10, 173 g/rod, in the 52a B_4C rods. The c/e for the edge rod in 48A were 1.04 to 1.07 depending on the calculational geometry. The main difference between the 48A calculations and the 52a calculations were the treatment of spatial self shielding of the poison cross sections and the high B-10 content.[7] Assembly 48A rod self-shielding calculations were made using 2DF X-Y models

TABLE 7. Natural B_4C and Tantalum Worth at Core Edge (P22)

Test Region	Excess Reactivity of Core (Ih)	Reactivity Change Relative to Void Ih)[a] Experiment	Calculation 2DB 8 Group X-Y	c/e
Reference	+ 15.3	0		
B_4C	-198.3	-214.3 ± 3.2	-213.0	0.99 ± 0.015
Ta	-106.0	-121.3 ± 2.0	-147.0	1.16 ± 0.019
B_4C/Ta Worth		1.78 ± 0.12	1.45	0.813 ± 0.055

(a) 1% $\Delta k/k$ = 1036 Ih[11]

in which actual rod geometries were specified in detail. The self-shielding calculations for poison rods in this work were made with flux-volume weighted cross sections which are described below.

The reactivity worth of a single peripheral tantalum drawer was calculated with a c/e of 1.213 ± 0.021 in 52a. The same rod was measured in the central column of 51 to be worth 573 Ih with a c/e of 0.935. Since tantalum has an appreciable resonance absorption component this element is more difficult to calculate than B-10.

Analyses of these experiments were done in X-Y geometry, using the two-dimensional diffusion code 2DB with an 8-group cross-section set. The control rod cross sections were flux-volume weighted to correct for heterogeneity. Flux-volume weightings were made with S-12 26-group DTF-IV cell calculations. The poison drawer cell was approximated with a one-dimensional slab model. In this case, the peripheral rod model, a slab core region and a slab reflector region were put on each side of the poison region. The principle traverse dimensions of the poison region were conserved as were average material concentrations. The poison was confined to a 1/2 in. thick region similar to the experiment. The average flux spectrum in the poison region was used to collapse the poison material cross

sections from 26 to 8 energy groups. A description of the calculational model for the cell calculation is given in Appendix B, Figure B-9.

The X-Y calculations were made with quarter core symmetry. This symmetry requires a minimum representation of two off center rods. Such a model was used and the answer was divided by two. In the analysis of Assembly 48A[5] it was shown that the error in this assumption is less than 1% of the measured worth of two core edge rods.

REFERENCES

1. E. R. Astley. Unpublished Data. Battelle-Northwest, Richland, Washington, May 23, 1968. (Letter to J. M. Shivley: Detailed Work Plan)

2. R. A. Bennett and P. L. Hofmann. Rationale and Plans for the FTR Critical Experiments Program, BNWL-490. Battelle-Northwest, Richland, Washington, June 1967.

3. W. R. Young and R. A. Bennett. Analysis of FTR Phase B Critical Experiments, Part 1, ZPR-III, Assembly 51, BNWL-1138. Battelle-Northwest, Richland, Washington, January 1970.

4. FFTF Reference Concept Summary Description, (Compiled by R. C. Walker) BNWL-955. Battelle-Northwest, Richland, Washington, June 1969.

5. Unpublished Data. (LMFBR Program Document No. 9) Physics Program.

6. R. A. Bennett, P. L. Hofmann, W. W. Little, and L. L. Maas. "Fast Test Reactor: Critical Experiments Program", Proc. of International Conference on Fast Critical Experiments and Their Analysis, ANL-7320. October 10-13, 1966.

7. R. A. Bennett and S. L. DeMyer. Analysis of FTR Phase A Control Rod Experiments in ZPR-III Assembly 48 and 48A, BNWL-967. Battelle-Northwest, Richland, Washington, April 1, 1969.

8. B. C. Cerutti, et al. "ZPR-III, Argonne's Fast Critical Facility," Nucl. Sci. Eng., vol 1, p. 126. 1956.

9. Reactor Development Program Progress Report, ANL-7403. Argonne National Laboratory, Argonne, Illinois, December 1967.

10. Reactor Development Program Progress Report, ANL-7460. Argonne National Laboratory, Argonne, Illinois, June 1968.

11. Reactor Development Program Progress Report, ANL-7445. Argonne National Laboratory, Argonne, Illinois, April 1968.

12. Reactor Development Program Progress Report, ANL-7478. Argonne National Laboratory, Argonne, Illinois, July 1968.

13. J. V. Nelson and S. L. DeMyer. Group Constants (Tape U1576) for Analysis of FFTF Critical Experiments, BNWL-1044. November 1969.

14. I. I. Bondarkeno, et al. "Group Constants for Nuclear Reactor Calculations," Consultants Bureau, New York, 1964.

15. R. W. Hardie and W. W. Little. FCC-IV, A Revised Version of the FCC Fundamental Mode Fast Reactor Code, BNWL-450. Battelle-Northwest, Richland, Washington, August 1967.

16. K. D. Lathrop. DTF-IV, A Fortran IV Program for Solving the Multigroup Transport Equation with Anisotopic Scattering, LA-3373. Los Alamos Scientific Laboratory, Los Alamos, N.M., July 15, 1965.

17. W. W. Little, and R. W. Hardie. 2DB, A Two-Dimensional Diffusion Burnup Code for Fast Reactor Analysis, BNWL-640. Battelle-Northwest, Richland, Washington, January 1968.

18. Unpublished Data. (2DF, A Two Dimensional Transport Code from the Los Alamos Scientific Laboratory)

19. R. W. Hardie and W. W. Little, Jr. PERT-IV, A Two-Dimensional Perturbation Code in FORTRAN-IV, BNWL-409, Battelle-Northwest, Richland, Washington, April 1967.

20. A. M. Broomfield, P. J. Amundson, W. G. Davey, J. M. Gasidlo, A. L. Hess, W. P. Keeney, and J. K. Long. "ZPR-3 Assembly 48: Studies of a Dilute Plutonium-fueled Assembly," Proceedings of the International Conference on Fast Critical Assembly Experiments and Their Analysis, p. 205, ANL-7320. Argonne National Laboratory, Argonne, Illinois, October 10-13, 1966.

21. G. I. Bell. "A Simple Treatment for Effective Resonance Absorption Cross Sections in Dense Lattices," Nuc. Sci. and Eng., vol 5, p. 138. 1959.

22. Reactor Development Program Progress Report, ANL-7513. Argonne National Laboratory, Argonne, Illinois, October 1968.

23. L. D. O'Dell, R. W. Hardie, and W. W. Little, Jr. A Numerical Comparison of Diffusion and Transport (S_n) Codes for Selected Fast Reactor Configurations, BNWL-922. Battelle-Northwest, Richland, Washington, March 1969.

24. Reactor Development Program Progress Report, ANL-7457. Argonne National Laboratory, Argonne, Illinois, May 1968.

25. Reactor Development Program Progress Report, ANL-7437. Argonne National Laboratory, Argonne, Illinois, August 1968.

APPENDIX A

CROSS SECTION ENERGY GROUP STRUCTURE

TABLE A-1. Energy Structure for 26-Group Cross-Section Set

Group	Fission Source	Energy Limit	Velocity	Delta σ
1	2.0000-02	6.5000+00	3.5311+09	4.8000-01
2	9.8000-02	4.0000+00	2.7700+09	4.8000-01
3	1.9000-01	2.5000+00	2.1899+09	4.8000-01
4	2.6800-01	1.4000+00	1.6388+09	5.7000-01
5	1.9600-01	8.0000-01	1.2388+09	5.7000-01
6	1.3500-01	4.0000-01	8.7595+08	6.9000-01
7	5.8000-02	2.0000-01	6.1939+08	6.9000-01
8	2.2000-02	1.0000-01	4.3798+08	6.9000-01
9	9.0000-03	4.6500-02	2.9866+08	7.7000-01
10	3.0000-03	2.1500-02	2.0308+08	7.7000-01
11	1.0000-03	1.0000-02	1.3850+08	7.7000-01
12	0.0000	4.6500-03	9.4444+07	7.7000-01
13		2.1500-03	6.4220+07	7.7000-01
14		1.0000-03	4.3798+07	7.7000-01
15		4.6500-04	2.9866+07	7.7000-01
16		2.1500-04	2.0308+07	7.7000-01
17		1.0000-04	1.3858+07	7.7000-01
18		4.8500-05	9.4444+06	7.7000-01
19		2.1500-05	6.4220+06	7.7000-01
20		1.0000-05	4.3798+06	7.7000-01
21		4.6500-06	2.9866+06	7.7000-01
22		2.1500-06	2.0308+06	7.7000-01
23		1.0000-06	1.3850+06	7.7000-01
24		4.6500-07	9.4444+05	7.7000-01
25		2.1500-07	6.4220+05	7.7000-01
26		2.5200-08	2.1986+05	7.7000-01
Sum	1.00000+00			

TABLE A-2. Energy Structure for 8-Group Cross-Section Set

New Group	Old Groups Per New Group	Fission Source For New Groups	Lower Energy Limit, MeV
1	3	3.08000-01	2.5
2	3	5.99000-01	0.4
3	3	8.90000-02	0.0465
4	3	4.00000-03	0.00465
5	2	0.00000	0.001
6	2	0.00000	0.000215
7	4	0.00000	0.00001
8	6	0.00000	0.0000000252

APPENDIX B

CALCULATIONAL MODELS

APPENDIX B

EXPLANATION OF CALCULATIONAL MODEL DATA SHEETS

Cross Section Sets

522226	Flux-volume weighted A-A* macroscopic core cross sections collapsed over central core zone fluxes to 8 energy groups
522326	Flux-volume weighted A-A* macroscopic core cross sections collapsed over out core zone fluxes to 8 energy groups
511921	Flux-volume weighted safety rod macroscopic cross sections collapsed over central core zone fluxes to 8 energy groups
FCC 74	8 group macroscopic radial reflector cross sections collapsed from central reflector fluxes
FCC 110	8 group macroscopic axial reflector cross sections collapsed from axial reflector fluxes
FCC 125	8 group macroscopic test zone cross sections collapsed from test zone fluxes
522427	Flux-volume weighted heavy safety rod macroscopic cross sections collapsed over safety rod, slab model, fluxes to 8 energy groups
522730	Flux-volume weighted tantalum rod macroscopic cross sections collapsed over tantalum rod, slab model, fluxes.

CALCULATION # 2DB58

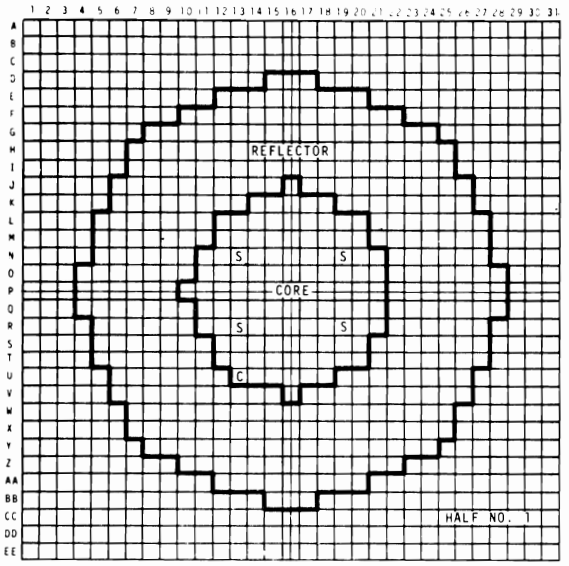

EXPERIMENTAL ASSEMBLY # 52a

EFFECTIVE CORE RADIUS _____

CORE HEIGHT _____

REFLECTOR THICKNESS { RADIAL _____ / AXIAL _____

CRITICAL MASS 200.7 kg

ABBREVIATIONS:

▨ _____ IN HALF #1, _____ IN HALF #2

[S] = SAFETY DRAWER

[C] = CONTROL DRAWER

▨ = ENRICHED DRAWER OF CELL

OTHER: _____

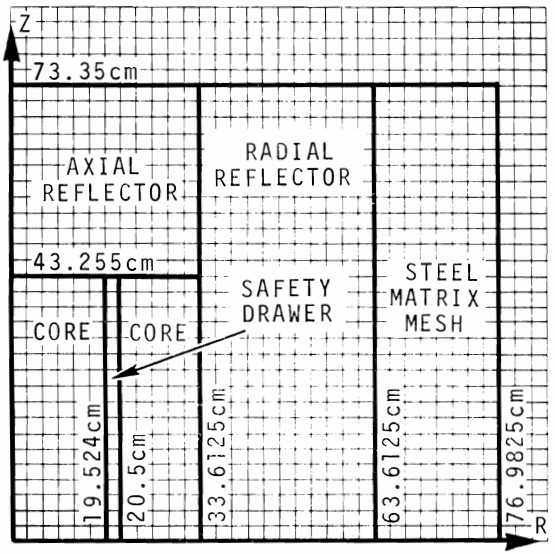

CALCULATIONAL MODEL

CODE 2DB GEOMETRY RZ

DIFFUSION _____, if S_N, N = _____

SYMMETRY 1/2 CORE

SOURCE OF ATOM DENSITIES _____

X-SECT. { GROUPS 8 / HOMO./HETERO. REFL/CORE

CORE HT. 86.51 cm

EFFECTIVE CORE RADIUS 32.006 cm

REFLECTOR THICKNESS RADIAL 30 cm / AXIAL 30 cm

BUCKLING 0

CALCULATED K_{eff} =	1.0000
CALCULATED MASS =	220.5 kg
CORE GAP	-0.0017
TEMPERATURE (NOT REPORTED)	0
SAFETY ROD POSITION	0
DIFFUSION → TRANSPORT S4	+0.0100
CYLINDRICIZATION OF SAFETY ROD AND CORE EDGE	
HOMOG. → HETEROGENEOUS	+0.0001
OTHER: A, A* IN ALTERNATE COLUMNS LESS 19.8 kg FISSILE AT CORE EDGE*	-0.00120 / -0.01742
CORRECTED DIFFUSION K_{eff}	0.9798
CORRECTED TRANSPORT K_{eff}	0.9898

ABBREVIATIONS:

[S] = SAFETY DRAWER

[C] = CONTROL DRAWER

OTHER:

MASS CORRECT :

CORRECTED MASS 200.7 kg

*Worth = 91.15 Ih/kg

FIGURE B-1

CALCULATION # 2DB124

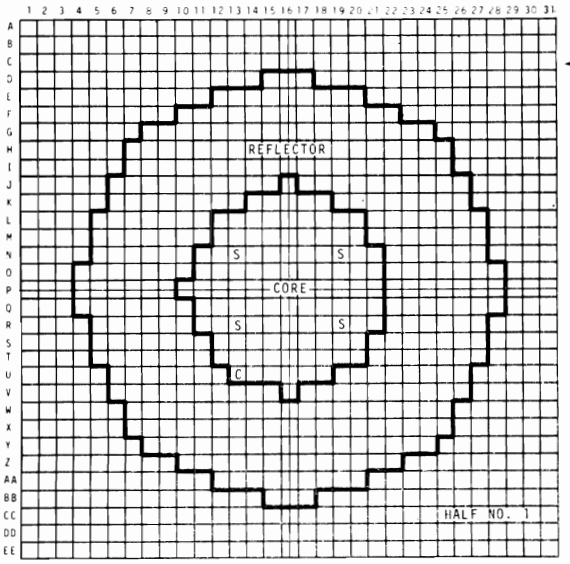

EXPERIMENTAL ASSEMBLY # 52a

EFFECTIVE CORE RADIUS _____

CORE HEIGHT _____

REFLECTOR THICKNESS { RADIAL _____ / AXIAL _____

CRITICAL MASS 200.7 ± 0.5 kg

ABBREVIATIONS:

[*] _____ IN HALF #1, _____ IN HALF #2

[S] = SAFETY DRAWER

[C] = CONTROL DRAWER

[/] = ENRICHED DRAWER OF CELL

OTHER: _____

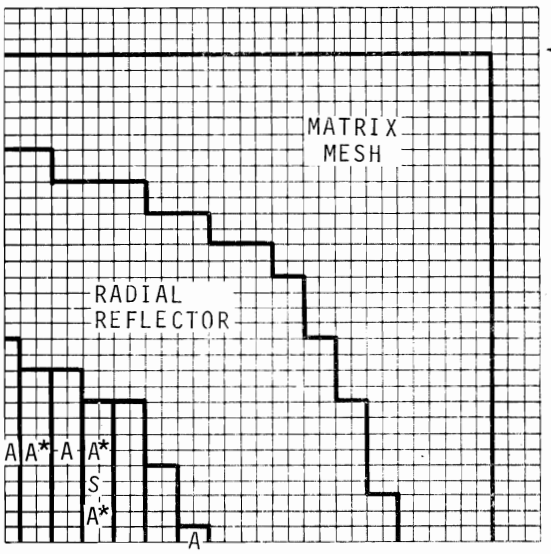

CALCULATIONAL MODEL

CODE 2DB GEOMETRY XY

DIFFUSION _____, if S_N, N = _____

SYMMETRY 1/4 CORE

SOURCE OF ATOM DENSITIES _____

X-SECT. { GROUPS 8 / HOMO./HETERO. REFL/CORE

CORE HT. 86.51 cm

EFFECTIVE CORE RADIUS 32.0 cm

REFLECTOR THICKNESS RADIAL 30 cm / AXIAL 30 cm

BUCKLING 6.85 m^{-2}

CALCULATED K_{eff} =	0.97805
CALCULATED MASS =	200.6 kg
CORE GAP	-0.0017
TEMPERATURE	0
SAFETY ROD POSITION	
DIFFUSION → TRANSPORT S4	0.01
HOMOG. → HETEROGENEOUS	
OTHER: ADD 0.1 AT CORE EDGE*	+0.00009

ABBREVIATIONS:

[S] = SAFETY DRAWER

[C] = CONTROL DRAWER

OTHER:

A = REGION WITH A TYPE DRAWERS

A* = REGION WITH A* TYPE DRAWERS

MASS CORRECT.:

CORRECTED MASS 200.7 kg

CORRECTED DIFFUSION K_{eff}	0.9764
CORRECTED TRANSPORT K_{eff}	0.9864

*93.24 lh/kg

FIGURE B-2

CALCULATION # 2DB32

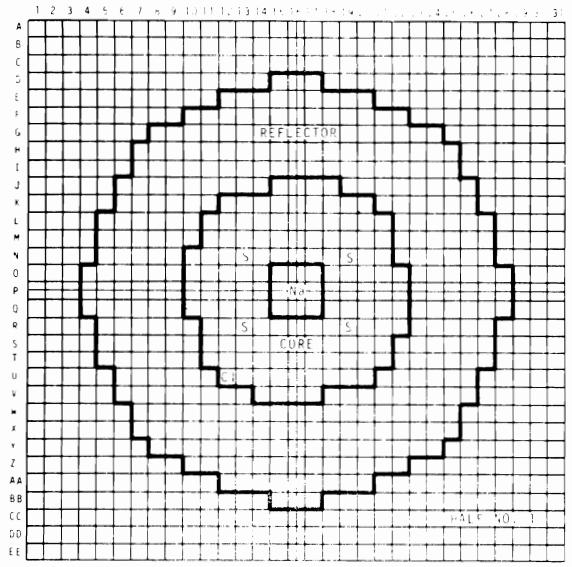

EXPERIMENTAL ASSEMBLY # 52B

EFFECTIVE CORE RADIUS _____

CORE HEIGHT _____

REFLECTOR THICKNESS { RADIAL _____ / AXIAL _____

CRITICAL MASS 235.9 ± 0.5 kg

ABBREVIATIONS:

▣ ____ IN HALF #1, ____ IN HALF #2

Ⓢ = SAFETY DRAWER

Ⓒ = CONTROL DRAWER

▨ = ENRICHED DRAWER OF CELL

OTHER: _____

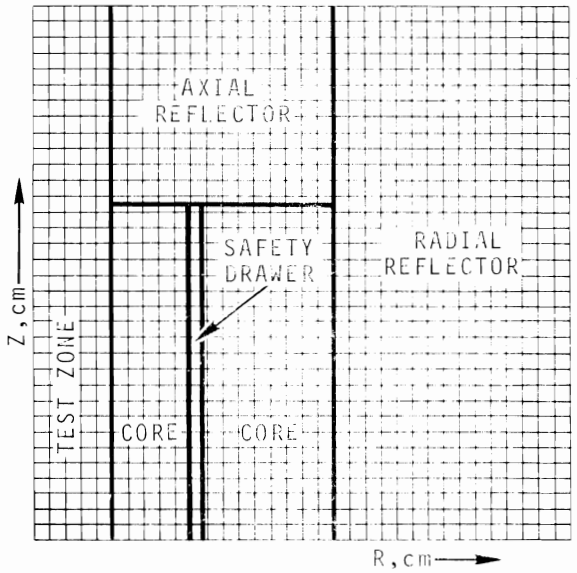

CALCULATIONAL MODEL

CODE 2DB GEOMETRY RZ

DIFFUSION _____, if S_N, N = _____

SYMMETRY 1/2 CORE

SOURCE OF ATOM DENSITIES _____

X-SECT. { GROUPS 8 / HOMO./HETERO. REFL/CORE

CORE HT. 86.51cm

EFFECTIVE CORE RADIUS 37.6344 cm

REFLECTOR THICKNESS { RADIAL 30 cm / AXIAL 30 cm

BUCKLING 0

CALCULATED K_{eff} =	1.0000
CALCULATED MASS =	258 kg
CORE GAP	-0.00200
TEMPERATURE	
SAFETY ROD POSITION	
DIFFUSION → TRANSPORT S4	0.00900
HOMOG. → HETEROGENEOUS	
OTHER:	
LESS 22 kg AT EDGE*	-0.01900
CORRECTED DIFFUSION K_{eff}	0.9790
CORRECTED TRANSPORT K_{eff}	0.9880

ABBREVIATIONS:

Ⓢ = SAFETY DRAWER

Ⓒ = CONTROL DRAWER

OTHER:

MASS CORRECT.:

CORRECTED MASS 236 kg

FIGURE B-3

CALCULATION # 2DB33

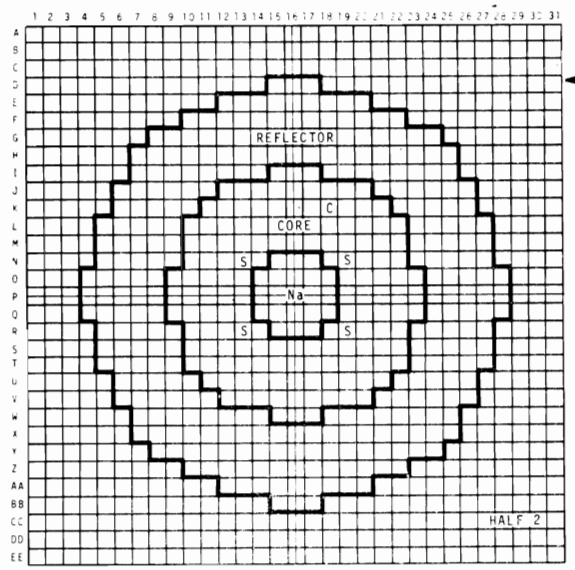

EXPERIMENTAL ASSEMBLY # 52C

EFFECTIVE CORE RADIUS _____

CORE HEIGHT _____

REFLECTOR THICKNESS { RADIAL _____ / AXIAL _____

CRITICAL MASS 280.0 ± 0.5 kg

ABBREVIATIONS:

▣ _____ IN HALF #1, _____ IN HALF #2

[S] = SAFETY DRAWER

[C] = CONTROL DRAWER

▨ = ENRICHED DRAWER OF CELL

OTHER: _____

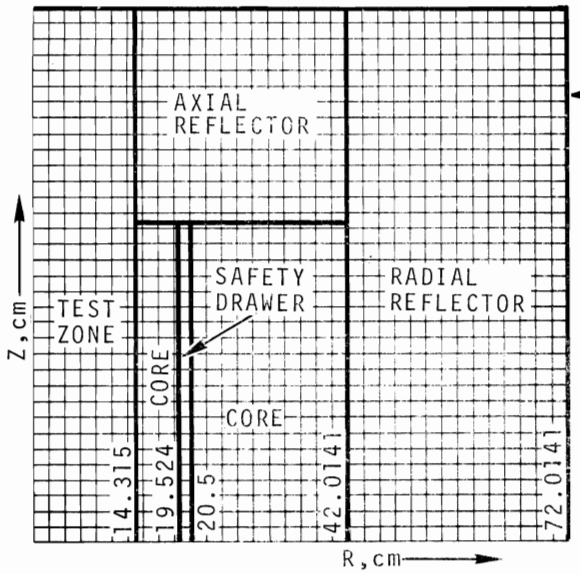

CALCULATIONAL MODEL

CODE 2DB GEOMETRY RZ

DIFFUSION _____, if S_N, N = _____

SYMMETRY 1/2

SOURCE OF ATOM DENSITIES _____

X-SECT. { GROUPS 8 / HOMO./HETERO. _____

CORE HT. 86.51 cm

EFFECTIVE CORE RADIUS 42.0141 cm

REFLECTOR THICKNESS { RADIAL 30 cm / AXIAL 30 cm

BUCKLING 0

CALCULATED K_{eff} = 1.000

CALCULATED MASS = 301 kg

CORE GAP -0.00170

TEMPERATURE _____

SAFETY ROD POSITION _____

DIFFUSION → TRANSPORT S_4 +0.00900

HOMOG. → HETEROGENEOUS _____

OTHER: _____

LESS 21 kg FISSILE AT EDGE* 0.01480

CORRECTED DIFFUSION K_{eff} 0.9835

CORRECTED TRANSPORT K_{eff} 0.9925

ABBREVIATIONS:

[S] = SAFETY DRAWER

[C] = CONTROL DRAWER

OTHER:

MASS CORRECT.:

CORRECTED MASS 280 kg

FIGURE B-4

CALCULATION # 2DB34

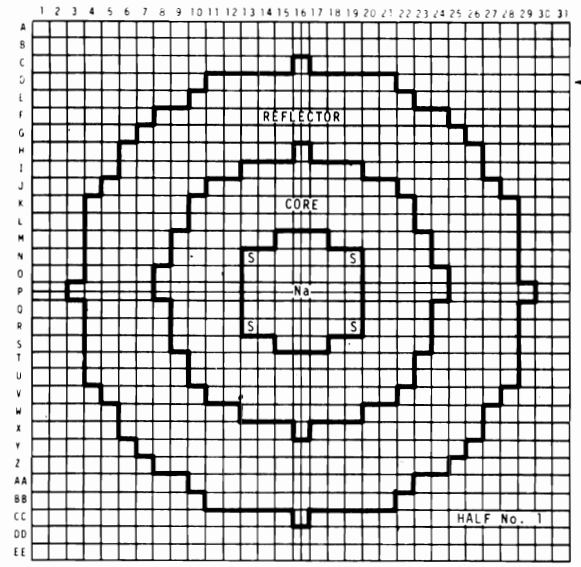

EXPERIMENTAL ASSEMBLY # 52F

EFFECTIVE CORE RADIUS _____

CORE HEIGHT _____

REFLECTOR THICKNESS { RADIAL _____ / AXIAL _____

CRITICAL MASS 309.2 ± 0.5 kg

ABBREVIATIONS:

[8] _____ IN HALF #1, _____ IN HALF #2

[S] = SAFETY DRAWER

[C] = CONTROL DRAWER

[/] = ENRICHED DRAWER OF CELL

OTHER: _____

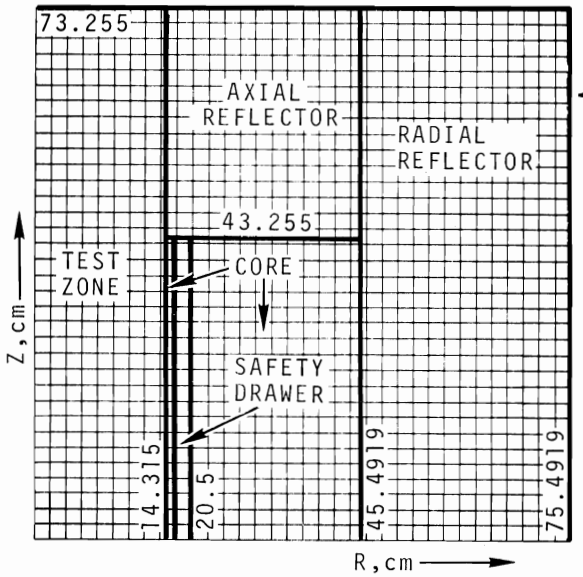

CALCULATIONAL MODEL

CODE 2DB GEOMETRY RZ

DIFFUSION _____, if S_N, N = _____

SYMMETRY 1/2

SOURCE OF ATOM DENSITIES _____

X-SECT. { GROUPS 8 / HOMO./HETERO. REFL/CORE

CORE HT. 86.511 cm

EFFECTIVE CORE RADIUS 45.4919 cm

REFLECTOR THICKNESS { RADIAL 30 cm / AXIAL 30 cm

BUCKLING 0

CALCULATED K_{eff} = 1.0000

CALCULATED MASS = 335.14 kg

CORE GAP -0.0017

TEMPERATURE 0

SAFETY ROD POSITION 0

DIFFUSION → TRANSPORT S 4 +0.0090

HOMOG. → HETEROGENEOUS _____

OTHER: _____

LESS 25.9 kg AT CORE EDGE* -0.0114

CORRECTED DIFFUSION K_{eff} 0.9869

CORRECTED TRANSPORT K_{eff} 0.9959

ABBREVIATIONS:

[S] = SAFETY DRAWER

[C] = CONTROL DRAWER

OTHER:

MASS CORRECT.:

CORRECTED MASS 309.2 kg

FIGURE B-5

CALCULATION # 2DB131

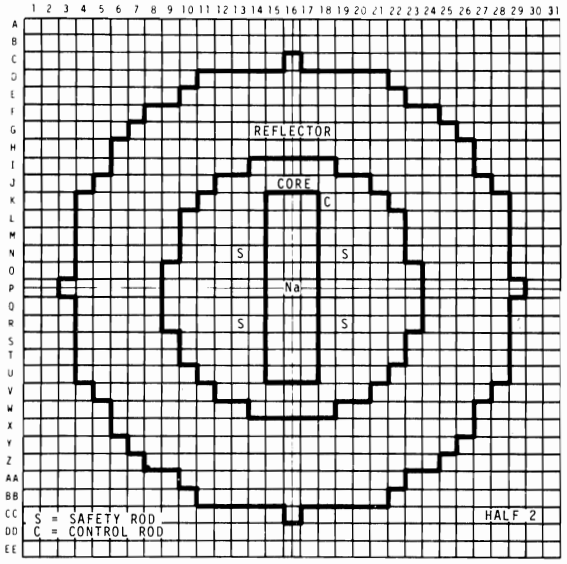

EXPERIMENTAL ASSEMBLY # 52D

EFFECTIVE CORE RADIUS _____

CORE HEIGHT _____

REFLECTOR THICKNESS { RADIAL _____ / AXIAL _____

CRITICAL MASS 275.2Kg

ABBREVIATIONS:

▣ _____ IN HALF #1, _____ IN HALF #2

[S] = SAFETY DRAWER

[C] = CONTROL DRAWER

⧄ = ENRICHED DRAWER OF CELL

OTHER: _____

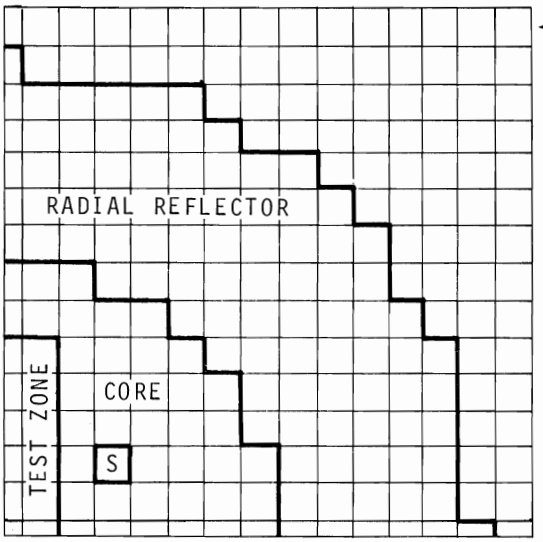

CALCULATIONAL MODEL

CODE 2 DB GEOMETRY X-Y

DIFFUSION _____, if S_N, N = _____

SYMMETRY 1/4

SOURCE OF ATOM DENSITIES _____

X-SECT. { GROUPS 8 / HOMO./HETERO. _____

CORE HT. 86.51

EFFECTIVE CORE RADIUS _____

REFLECTOR THICKNESS RADIAL 30 cm / AXIAL 30 cm

BUCKLING 6.85 CORE, 4.54 TEST m^{-2}

ABBREVIATIONS:

[S] = SAFETY DRAWER

[C] = CONTROL DRAWER

OTHER:

MASS CORRECT.:

CORRECTED MASS 275.2 kg

CALCULATED K_{eff} =	0.98246
CALCULATED MASS =	279.03 kg
CORE GAP	-0.0017
TEMPERATURE	
SAFETY ROD POSITION	
DIFFUSION → TRANSPORT S	+0.009
HOMOG. → HETEROGENEOUS	
OTHER: LESS 3.83 AT CORE EDGE*	-0.00270
CORRECTED DIFFUSION K_{eff}	0.9788
CORRECTED TRANSPORT K_{eff}	0.9878

FIGURE B-6

CALCULATION # 2DB129

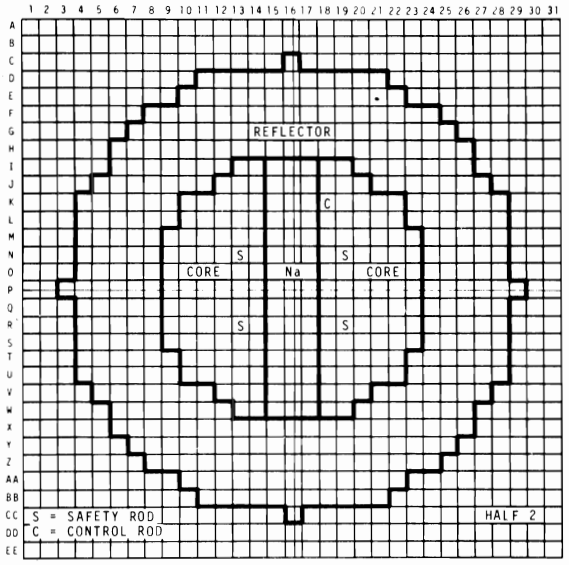

EXPERIMENTAL ASSEMBLY # 52e

EFFECTIVE CORE RADIUS _____

CORE HEIGHT _____

REFLECTOR THICKNESS { RADIAL _____ / AXIAL _____

CRITICAL MASS 282.0 ± 1.9 kg

ABBREVIATIONS:

▣ _____ IN HALF #1, _____ IN HALF #2

Ⓢ = SAFETY DRAWER

Ⓒ = CONTROL DRAWER

◪ = ENRICHED DRAWER OF CELL

OTHER: _____

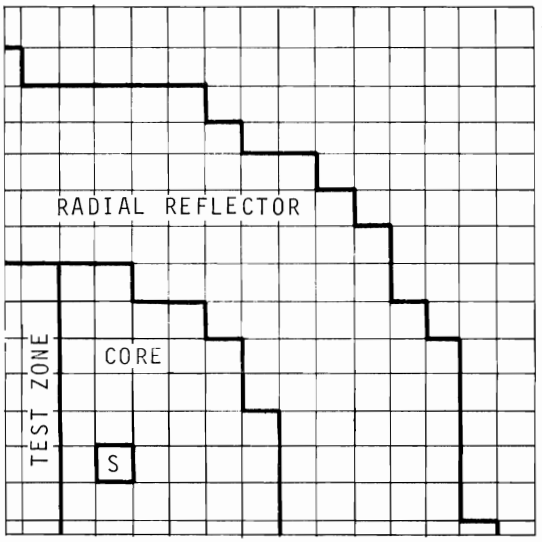

CALCULATIONAL MODEL

CODE _____ GEOMETRY _____

DIFFUSION _____, if S_N, N = _____

SYMMETRY _____

SOURCE OF ATOM DENSITIES _____

X-SECT. { GROUPS 8 / HOMO./HETERO. _____

CORE HT. 86.51 cm

EFFECTIVE CORE RADIUS _____

REFLECTOR THICKNESS RADIAL 30 cm / AXIAL 30 cm

BUCKLING 6.85 m^{-2} CORE, 4.54 m^{-2} TEST

CALCULATED K_{eff} = 0.98311

CALCULATED MASS = 269.3

CORE GAP -0.0017

TEMPERATURE _____

SAFETY ROD POSITION _____

DIFFUSION → TRANSPORT S 4 +0.00900

HOMOG. → HETEROGENEOUS _____

OTHER: *+0.0062 / -0.0004

ABBREVIATIONS:

Ⓢ = SAFETY DRAWER

Ⓒ = CONTROL DRAWER

OTHER:

MASS CORRECT.:

CORRECTED MASS 282 kg

CORRECTED DIFFUSION K_{eff} _____

CORRECTED TRANSPORT K_{eff} _____

*50.58 Ih/kg

FIGURE B-7

CALCULATION # 2DB59

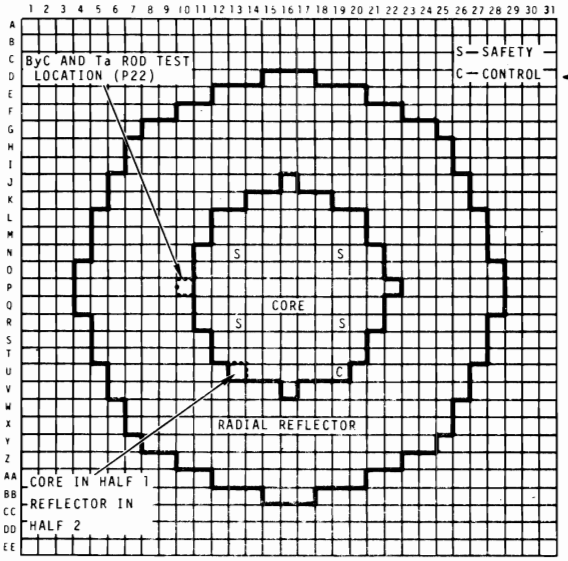

EXPERIMENTAL ASSEMBLY #

EFFECTIVE CORE RADIUS _____

CORE HEIGHT _____

REFLECTOR THICKNESS { RADIAL _____ / AXIAL _____

CRITICAL MASS _____

ABBREVIATIONS:

[*] _____ IN HALF #1, _____ IN HALF #2

[S] = SAFETY DRAWER

[C] = CONTROL DRAWER

[/] = ENRICHED DRAWER OF CELL

OTHER: _____

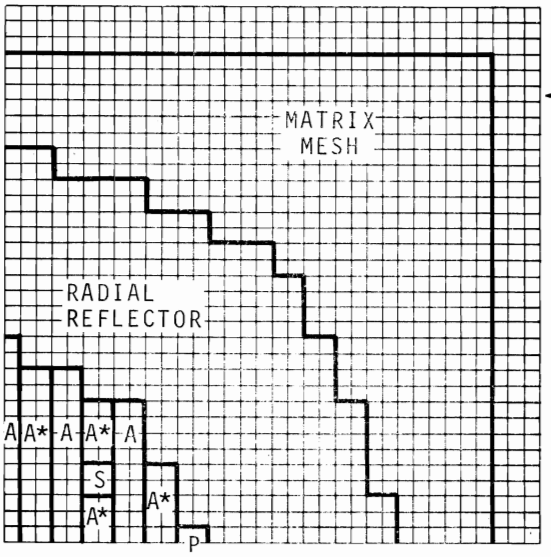

CALCULATIONAL MODEL

CODE 2DB GEOMETRY XY

DIFFUSION _____, if S_N, N = _____

SYMMETRY 1/4 CORE

SOURCE OF ATOM DENSITIES _____

X-SECT. { GROUPS 8 / HOMO./HETERO. REFL/CORE

CORE HT. _____

EFFECTIVE CORE RADIUS _____

REFLECTOR THICKNESS { RADIAL _____ / AXIAL _____

BUCKLING 5.06 m^{-2}

CALCULATED K_{eff} = 1.000(RODS OUT)

CALCULATED MASS = 197 kg

ABBREVIATIONS:

[S] = SAFETY DRAWER

[C] = CONTROL DRAWER

OTHER:

P= PERIPHERAL POISON DRAWER
A= REGION WITH "A" CORE DRAWERS
A* =REGION WITH "A*" CORE DRAWERS

MASS CORRECT.:

CORRECTED MASS 197 kg

CORE GAP _____

TEMPERATURE _____

SAFETY ROD POSITION _____

DIFFUSION → TRANSPORT S _____

HOMOG. → HETEROGENEOUS _____

OTHER: _____

CORRECTED DIFFUSION K_{eff} _____

CORRECTED TRANSPORT K_{eff} _____

FIGURE B-8

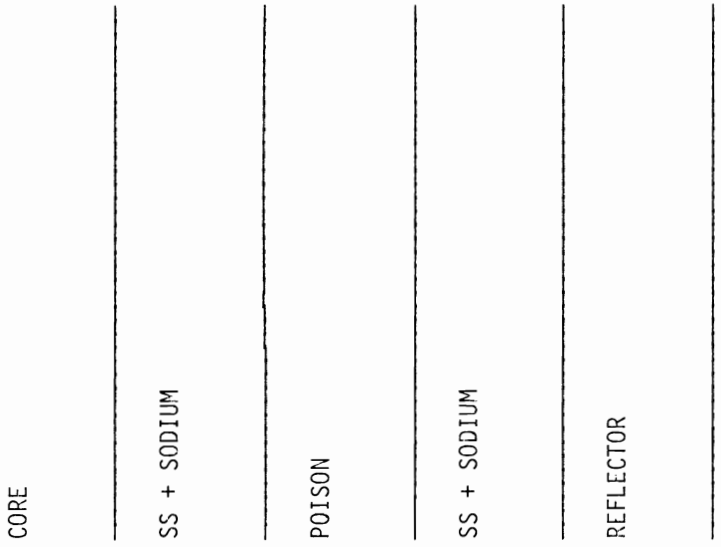

CALCULATIONAL MODEL

CODE: DTF-IV (Modified)

GEOMETRY: ID Slab

BOUNDARY CONDITIONS: Left, Reflecting
Right, Vacuum

SN: 12

ENERGY GROUPS: 26

FLUX-VOLUME WEIGHTING OVER
SODIUM AND POISON ZONES

REGION	ATOM DENSITIES 10^{24} ATOM ICC	REGION THICKNESS, CM
Core		
Average Concentrations, A-A* Cell, Table I		33.0
SS + Sodium		
Fe	0.03017	2.138
Cr	0.007881	
Ni	0.003103	
Na	0.010835	
Poison		
B_4C		1.27
B-10	0.015965	
B-11	0.067993	
C	0.02266	
Or		
Tantalum		
Ta	0.04885	
Reflector		
Radial Reflector Concentrations, Table I		30.0

FIGURE B-9. Calculational Model for Peripheral Poison Rod Cell Calculation, Assembly 52a

DISTRIBUTION

No. of Copies

OFFSITE

1 AEC Chicago Patent Group
G. H. Lee

31 AEC Division of Reactor Development and Technology
M. Shaw, Director, RDT
Asst Dir for Nuclear Safety
Analysis & Evaluation Br, RDT:NS
Environmental & Sanitary Engrg Br, RDT:NS
Research & Development Br, RDT:NS
Asst Dir for Plant Engrg, RDT
Facilities Br, RDT:PE
Components Br, RDT:PE
Instrumentation & Control Br, RDT:PE
Liquid Metal Systems Br, RDT:PE
Asst Dir for Program Analysis, RDT
Asst Dir for Project Mgmt, RDT
Liquid Metals Projects Br, RDT:PM
FFTF Project Manager, RDT:PM (3)
Asst Dir for Reactor Engrg, RDT
Control Mechanisms Br, RDT:RE
Core Design Br, RDT:RE (2)
Fuel Engineering Br, RDT:RE
Fuel Handling Br, RDT:RE
Reactor Vessels Br, RDT:RE
Asst Dir for Reactor Tech, RDT
Coolant Chemistry Br, RDT:RT
Fuel Recycle Br, RDT:RT
Fuels & Materials Br, RDT:RT
Reactor Physics Br, RDT:RE
Special Technology Br, RDT:RT
Asst Dir for Engrg Standards, RDT
EBR-II Project Manager, RDT:PM

197 AEC Division of Technical Information Extension

1 AEC Idaho Operations Office
Nuclear Technology Division
C. W. Bills, Director

1 AEC San Francisco Operations Office
Director, Reactor Division

No. of Copies

4 AEC Site Representatives

Argonne National Laboratory
Atomics International
General Electric Company
Westinghouse Electric Corporation

3 Argonne National Laboratory

R. A. Jaross
LMFBR Program Office
N. J. Swanson

1 Atomic Power Development Assoc.

Document Librarian

5 Atomics International

FFTF Program Office

2 Babcock & Wilcox Company
Atomic Energy Division

S. H. Esleeck
G. B. Garton

10 Bechtel Corporation

J. J. Teachnor, Project Administrator, FFTF

1 BNW Representative

R. M. Fleischman (ZPR-9)

1 Combustion Engineering
1000 MWe Follow-On Study

W. P. Staker, Project Manager

1 Combustion Engineering
911 West Main Street
Chattanooga, Tennessee 37401

Mrs. Nell Holder

5 General Electric Company
Advanced Products Operation

Karl Cohen (4)

Nuclear Systems Programs

D. H. Ahmann

No. of Copies	
2	Gulf General Atomic Inc. General Atomic Division D. Coburn
1	Idaho Nuclear Corporation J. A. Buckham
1	Liquid Metal Engineering Center R. W. Dickinson
2	Liquid Metal Information Center A. E. Miller
1	Oak Ridge National Laboratory W. O. Harms
1	Stanford University Nuclear Division Division of Mechanical Engrg R. Sher
1	United Nuclear Corporation Research and Engineering Center R. F. DeAngelis
15	Westinghouse Electric Corporation Atomic Power Division Advanced Reactor Systems J. C. R. Kelly

ONSITE—HANFORD

1	AEC Chicago Patent Group R. K. Sharp
4	AEC RDT Site Representatives P. G. Holsted (3) T. A. Nemzek
2	AEC Richland Operations Office J. M. Shivley

No. of Copies

3 Battelle Memorial Institute

1 Bechtel Corporation

M. O. Rothwell (Richland)

1 Westinghouse Electric Corporation

R. Strzelecki (Richland)

78 Battelle-Northwest

E. R. Astley
Q. L. Baird
A. L. Bement
R. A. Bennett
E. T. Boulette
W. L. Bunch
W. L. Chase
J. C. Cochran
D. L. Condotta
S. L. DeMyer
J. F. Erben
E. A. Evans
C. L. Fies
J. W. Hagan
R. W. Hardie
P. L. Hofmann
H. E. Little
W. W. Little
C. A. Mansius
D. R. Marr
W. B. McDonald
J. S. McMahon
J. V. Nelson
L. D. O'Dell
R. P. Omberg
H. C. R. Ripfel
J. M. Seehuus
J. R. Sheff
R. J. Squires
D. D. Stepnewski
A. E. Waltar
J. H. Westsik
B. Wolfe
W. R. Young (25)

Legal-703 Bldg.
Legal-ROB, 221-A
Technical Information (5)
Technical Publications (2)
FFTF File (703) (10)
FFTF TPO (703)